frontiers in Soil Science

TYPE Original Research
PUBLISHED 03 March 2026
DOI 10.3389/fsoil.2026.1754030

OPEN ACCESS

EDITED BY
Layla M. San-Emeterio,
Swedish University of Agricultural Sciences, Sweden

REVIEWED BY
Xiaoming Wan,
Chinese Academy of Sciences (CAS), China
Maochao Zhang,
Qingyuan Polytechnic, China

*CORRESPONDENCE
Otávio Anjos Leal
o.dos.anjos.leal@fz-juelich.de

RECEIVED 11 December 2025
REVISED 02 February 2026
ACCEPTED 09 February 2026
PUBLISHED 03 March 2026

CITATION
Oliveira JR, Fernandez MBG, Leal OA, Brisolara BL, Ribeiro AS, Gomes CG, Pinto LFS, Job MTP and Stumpf L (2026) Environmental, ecological and human health risk assessment for Ba, Cr, Zn and V in minesoil after 20 years of restoration in southern Brazil. *Front. Soil Sci.* 6:1754030. doi: 10.3389/fsoil.2026.1754030

Environmental, ecological and human health risk assessment for Ba, Cr, Zn and V in minesoil after 20 years of restoration in southern Brazil

Jakeline Rosa Oliveira[1], Maria Bertaso Garcia Fernandez[1], Otávio Anjos Leal[2]*, Bruna Lemons Brisolara[1], Anderson Schwingel Ribeiro[3], Charlie Guimarães Gomes[3], Luiz Fernando Spinelli Pinto[1], Marcel Thomas Pereira Job[1] and Lizete Stumpf[1]

[1]Soil and Water Management and Conservation Program (MACSA), Soil department, Federal University of Pelotas (UFPel), Pelotas, Brazil, [2]Institute of Bio- and Geosciences - Agrosphere (IBG-3), Forschungszentrum Jülich GmbH, Jülich, Germany, [3]Program in Chemistry Chemical Metrology Laboratory (LabMeQui), Federal University of Pelotas (UFPel), Pelotas, Brazil

Heavy metals are a persistent threat in soils formed after mining (minesoils). This study was conducted in a 20-year randomized complete block design experiment installed within an active coal mine in Candiota, southern Brazil. Thus, this work provides a unique opportunity to assess long-term environmental and human health risks as affected by consistent and well-documented minesoil restoration practices. We aimed to assess the concentration of heavy metals (Zn, V, Ba, and Cr) in topsoil layers (0.00–0.10 and 0.10–0.20 m) and their associated ecological (with emphasis on soil fauna), environmental and human health risk as function of grass species used for revegetation of the minesoil (*Hemarthria altissima*, *Cynodon dactylon*, and *Urochloa brizantha*). Overall, Cr concentrations exceeded the regional quality reference value (25 mg kg^{-1}), regardless of grass species and soil layer, despite 20 years of permanent revegetation. According to the pollution index (PI), the minesoil was classified as "moderately polluted" for Ba and Cr and as "severely polluted" for V, particularly under *H. altissima* (PI for V = 3.22 and Ba = 2.17). Among grass species, *U. brizantha* resulted in the lowest PI and ecological risk values and supported the highest abundance of soil fauna (2,309 individuals), compared to *C. dactylon* (2,075) and *H. altissima* (1,714). The human health risk assessment indicated "ingestion" as the main exposure pathway for adults, while "inhalation" accounted for approximately 75% of the total hazard index for children. Our findings highlight the persistent environmental and human health risks in the coal minesoils in Candiota, Brazil, even after 20 years of restoration. We strongly recommend the continued monitoring of these parameters to protect people and environment in Candiota region against contamination by heavy metals.

KEYWORDS
hazard quotient, non-carcinogenic and carcinogenic risk, perennial grasses, pollution index, soil fauna indexes

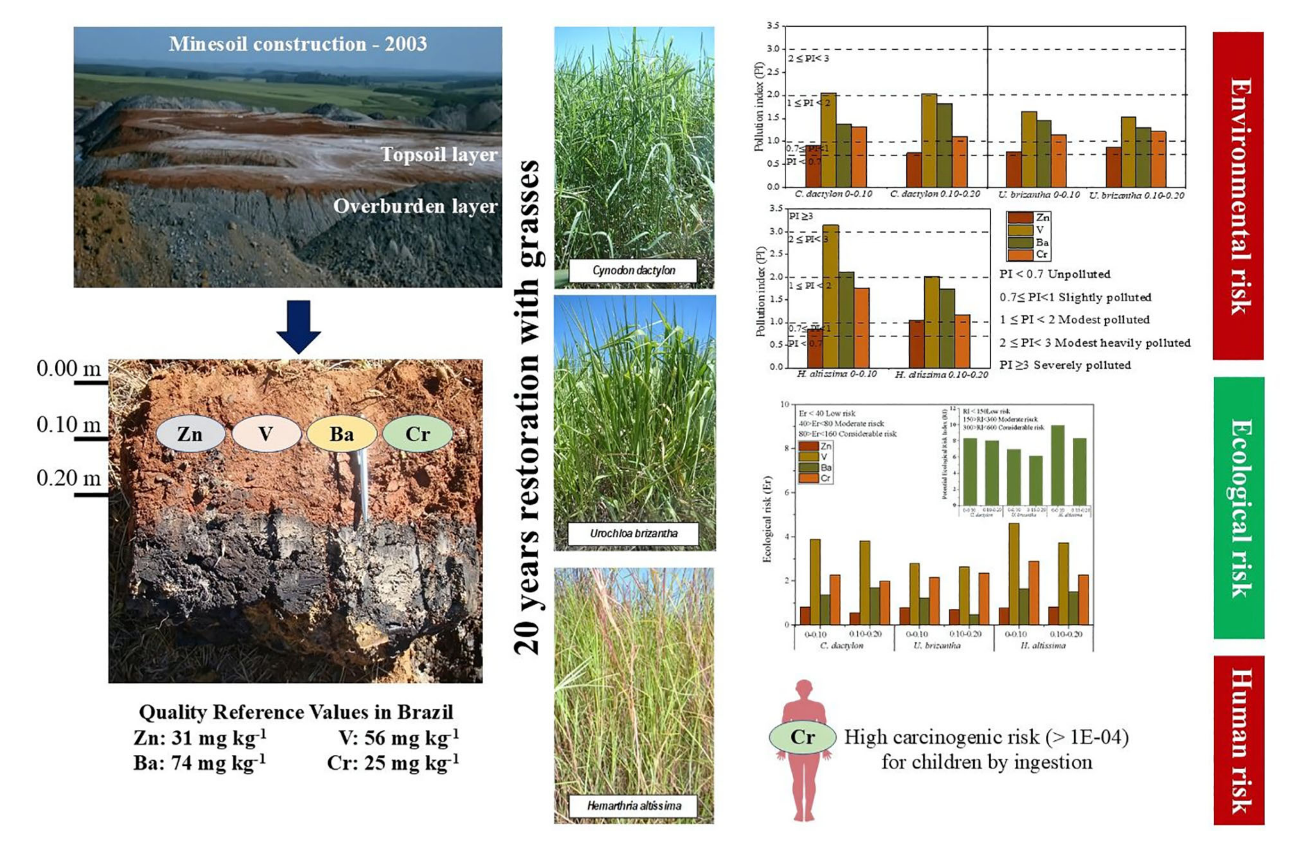

GRAPHICAL ABSTRACT

1 Introduction

Brazil holds the tenth-largest mineral coal reserve in the world. The state of Rio Grande do Sul (RS), located in the southern region of the country, accounts for over 90% of the nation's coal reserves, mainly represented by the Candiota deposit (about 1.2 billion tons), where mining is open-pit (1). Even after topographic restoration and long-term vegetation regeneration, studies worldwide indicate that soils in mining areas may contain elevated concentrations of heavy metals (HMs) such as As, Ba, Cd, Cr, Cu, Hg, Ni, Pb, Zn, V, Fe, Al, and Mn (2–5).

Heavy metals can either be dispersed across long distances through water or wind erosion or persist locally as residual deposits (6–11). According to their physiological functions, certain HMs are considered essential (such as Co, Cu, Mn, Mo, Ni, and Zn), because they participate directly in plant metabolic processes (12). In contrast, other HMs (including As, Cd, Cr, Hg, V, Ba, and Pb) are regarded as non-essential, as they have no known metabolic role in plants and are generally toxic to living organisms even at low concentrations (13, 14). Soil serves as the main reservoir for HMs released into the environment, where they can remain stable over long time spans, from several decades to even thousands of years (14). Most HMs are not significantly transformed by microbial or chemical processes. Instead, they undergo only limited modifications in their chemical speciation and bioavailability (15, 16). Consequently, these elements tend to accumulate in the soil in the long-term and to interfere in the morphological structure and physiological processes of soil fauna as well as in plant metabolism (17).

The quality of the residues of the plants used for environmental restoration of mined areas plays a critical role in driving the return of soil fauna communities and ecological restoration of the mined area (18–20). In mined areas, plant residues may be contaminated with HMs, thereby affecting fauna functions, such as biomass decomposition. Wierzbicka et al. (21) observed that the abundance of biomass-decomposing organisms, such as mites (oribatids) responded negatively to elevated concentrations of Pb, Zn, Cd, and Cu in the plant residues of Scots pine (*Pinus sylvestris* L.) growing in heavily HM-polluted areas in Poland. Even moderate residual levels of HMs may present risks depending on their bioavailability, persistence, and ecological context.

Specifically, in the Candiota coal mine in southern Brazil, responses of soil fauna to soil pollution remain unstudied, and such studies are urgently needed. Beyond the effects of HMs on soil biological communities, HMs can ultimately enter the human body, either through direct contact with contaminated soil or indirectly via the food chain, posing a significant threat to public health (9). According to the World Health Organization, in 2012 about 12.6 million deaths globally (approximately 23% of all deaths) were attributed to harmful environment, including HMs, and for children under five years, up to 26% of deaths could have been prevented by the removal of environmental risks (22). This is related to the non-biodegradable nature of HMs, which leads to increasing levels of environmental contamination, human exposure to these toxic elements, and bioaccumulation of HMs at various trophic levels (23–25). Therefore, comprehensive studies on harmful impacts of HMs to society are a priority, especially in developing countries because of their greatest share of environmental diseases (22).

The efficient management of areas affected by HMs requires a diverse range of methodologies to adequately identify and quantify individual and integrated impacts of the HMs studied. Pollution indicators, such as the contamination factor (CF), pollution index (PI), and potential ecological risk index (RI), have been widely applied to assess ecosystem risks associated with soil pollution by HMs (26–30). Furthermore, human health risk assessment is a valuable tool for revealing non-carcinogenic (HQ) and carcinogenic (CR) risks posed by organic and inorganic pollutants across various environmental media and for different age groups (29, 31, 32).

The selection of the metals V, Cr, Ba, and Zn is based on their recurrent presence in areas affected by coal mining, where they are commonly associated with local geology, mining waste, and acid mine drainage (33–35). In the case of the Candiota mine, it is noteworthy that the concentrations of Cr, V, and Ba still exceed the reference values established by the environmental legislation of RS State, Brazil (36), even after two decades of soil restoration with perennial grasses. This suggests the persistence of contamination and validates the application of ecological and health risk assessment methodologies.

Our study was conducted within a long-term (20-year) field experiment located inside an active coal mine, which allowed for consistent sampling over time in controlled conditions a rare opportunity in environmental field studies. This experimental design strengthens the temporal comparisons and enhances the reliability of the observed impacts associated with revegetation strategies. This article focuses primarily on two objectives (1): determining the concentrations of Zn, V, Ba, and Cr in the minesoil cultivated with *Hemarthria altissima*, *Cynodon dactylon*, and *Urochloa brizantha* at topsoil layers (0.00–0.10 and 0.10–0.20 m; and (2) evaluating the environmental, ecological (with an emphasis on soil fauna), and human health risks associated with these HMs in the restored minesoil. Based on previous studies highlighting distinguishable effects of these grasses on soil quality and fauna communities (37–42), we hypothesized that the concentration of HMs in the minesoil and investigated risks may differ depending on the grass species used for minesoil revegetation.

2 Materials and methods

2.1 Experimental area history

The study was conducted in the Candiota coal mine area, located in the state of RS, southern Brazil (Figure 1). This is an active coal mining area operating since 1961. The climate is subtropical humid (Cfa), the average annual temperature is 17 °C and average annual rainfall is 1,400 mm, including a cold winter and a hot summer (43). The coal mine is located in the Pampa Biome, characterized by its slightly undulated topography and grassland vegetation (44). Therefore, most of the soils mined to date, including those in our experimental area, were mined under these conditions.

The experimental area was set up in November/December 2003 in a randomized complete block design with four replicates (plots of 4 x 5 m). Before grass planting, 84 samples of the topsoil were taken across the experimental area for organic carbon content and texture determination to ensure a proper arrangement of the four

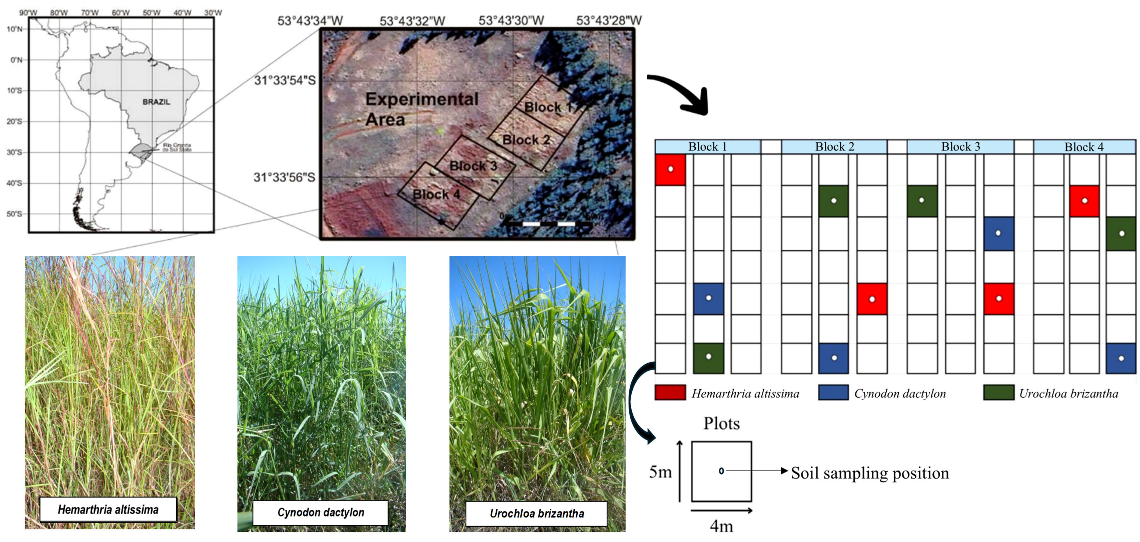

FIGURE 1
Location and layout of the minesoil field experiment established at the Candiota Coal Mine, southern Brazil. The map shows the regional location of the study area, while the aerial image illustrates the experimental design with four randomized blocks and plots (4 × 5 m) restored with perennial grasses (*Cynodon dactylon*, *Urochloa brizantha*, and *Hemarthria altissima*).

experimental blocks (Figure 1). The four blocks addressed the terrain's slope. On the same occasion, the natural soil (unmined) was sampled and characterized. The topsoil of the four blocks of the experimental area exhibited a 2.5YR color, clay content from 448 to 455 g kg^{-1} and organic carbon content between 4.9 and 5.6 g kg^{-1}, which are consistent with characteristics of the B horizon of the natural soil (Table 1). Therefore, it is inferred that the topsoil of the minesoil (approx. 40 cm) consists mostly of the B-horizon of the natural (pre-mining) soil, which is typically placed over the overburden layer in this area (40).

Before grass planting, the topsoil was chiseled with a bulldozer to a 0.15 m depth as it exhibited signs of severe compaction exerted by the traffic of heavy machinery used for topographic recomposition of the landscape. On this occasion, soil pH corrections and fertilization were performed using dolomitic limestone (10.4 Mg ha^{-1}) and 900 kg ha^{-1} of a 5–20–20 fertilizer (45 kg N, 180 kg P_2O_5, and 180 kg K_2O), based on results of soil analysis.

Several grass and legume species were tested as monoculture or as consortia, as described in Stumpf et al. (45). In the present study, results refer to monoculture of three perennial grasses of the Poaceae Family, which were planted through seedlings in November/December 2003: *Hemarthria altissima* (Poir.) Stapf & C.E. Hubbard, *Cynodon dactylon* (L.) Pers. cv. Tifton, and *Urochloa brizantha* (Hochst. ex A. Rich.) Stapf. No mowing of the aboveground biomass of the grasses and no irrigation was performed on the plots analyzed, resembling the management adopted by the mining company.

The only practice adopted between 2003 and 2023, generally in the autumn/winter period, was broadcast fertilization. Thus, every year since its implementation, all plots of the experiment received 250 kg ha^{-1} of a 5–30–15 fertilizer (12.5 kg N, 75 kg P_2O_5, and 37.5 kg K_2O) and 250 kg ha^{-1} of urea. Fertilization was carried out based on our Fertilization and Liming Manual for soils in Rio Grande do Sul and Santa Catarina (46) to ensure the maintenance of the chemical quality of this soil throughout the experiment.

TABLE 1 **Physico-chemical characterization of minesoil after the reconstruction of the soil profile and the natural soil of the mining front (40).**

Soil	Blocks or Horizons	Clay (g kg^{-1})	Organic carbon (g kg^{-1})	Color
Minesoil Experimental area	Block 1	455	4.9	2YR
	Block 2	448	5.5	
	Block 3	450	4.4	
	Block 4	455	5.6	
Natural Soil Rodic Lixisol	Hz A	231	11.0	5YR
	Hz AB	340	8.0	
	Hz BA	402	6.0	2YR
	Hz Bt1	550	5.0	
	Hz Bt2	470	3.0	
	Hz BC	445	3.0	

2.2 Minesoil chemical and physical characterization at 20 years of restoration

The basic soil chemical and physical attributes (0.00–0.10 and 0.10–0.20 m layer) in each treatment after 20 years of restoration are provided in Table 2. The soil pH was determined in water at a ratio of 1:1 (soil:water, w:v). Exchangeable calcium (Ca^{2+}), magnesium (Mg^{2+}), and aluminum (Al^{3+}) were extracted with 1 mol L^{-1} KCl and Ca and Mg were analyzed using a flame atomic absorption spectrophotometer (GBC model SAVANTAA) with an air/acetylene flame ratio of 10:1. The quantification of Al present in the samples was performed by titration using NaOH. Available potassium (K^+) was extracted with the Mehlich^{-1} method and analyzed by flame photometry (EleveLab, model EL-6400). Potential acidity (H+Al) was determined by titration with NaOH after extraction with calcium acetate. Soil total organic carbon (TOC) content was determined by the Walkley-Black combustion method. These analyses were performed according to Teixeira et al. (47). The pH values observed across treatments and soil layers (5.55 to 6.11) likely reflect the long-term positive effect of soil liming conducted in 2003. These values remain close to or higher than the reference value (pH > 5.5) for perennial summer grasses according to regional recommendations (46).

The soil organic matter contents observed in the minesoil are considered medium (2.6–5.0%) in the 0.00–0.10 m layer and low (≤

TABLE 2 **Minesoil chemical and physical attributes at 0.00–0.10 and 0.10–0.20 m layer after 20 years of restoration with three perennial grasses (*Cynodon dactylon*, *Urochloa brizantha* and *Hemarthria altissima*).**

Chemical attributes	*Hemarthria altissima*	*Urochloa brizantha*	*Cynodon dactylon*
0.00–0.10 m			
pH (H_2O)	5.87	5.55	5.86
Ca (cmolc kg^{-1})	5.76	4.89	5.63
Mg (cmolc kg^{-1})	1.06	2.61	1.09
H+Al (cmolc kg^{-1})	6.13	11.92	6.81
K (cmolc kg^{-1})	0.33	0.53	0.41
OM (%)	3.6	4.2	3.5
Bd (Mg m^{-3})	1.31	1.27	1.37
Ma (m^3 m^{-3})	0.10	0.15	0.12
Tp (m^3 m^{-3})	0.50	0.57	0.50
0.10–0.20 m			
pH (H_2O)	6.11	5.68	5.65
Ca (cmolc kg^{-1})	5.44	4.72	3.49
Mg (cmolc kg^{-1})	1.00	2.31	0.77
H+Al (cmolc kg^{-1})	5.88	9.81	9.79
K (cmolc kg^{-1})	0.19	0.28	0.23
OM (%)	2.4	2.4	1.7
Bd (Mg m^{-3})	1.46	1.38	1.59
Ma (m^3 m^{-3})	0.08	0.11	0.08
Tp (m^3 m^{-3})	0.45	0.48	0.40

Adapted from Fernandes et al. (2025). Ca: calcium; Mg: magnesium; H+ Al: potential acidity; K: potassium; OM: organic matter; Bd: bulk density; Ma: macroporosity; Tp: total porosity.

2.5%) in the 0.10–0.20 m layer according to CQFS (46). The higher organic matter values in the upper minesoil layer are reflected in the lower bulk density (Bd) values (1.27 to 1.37 Mg m^{-3}) and higher macroporosity (Ma) volumes (0.10–0.15 m^3 m^{-3}) compared to the underlying layer (Bd between 1.38 and 1.59 Mg m^{-3} and Ma between 0.08–0.11 m^3 m^{-3}). These results are published in Fernandes et al. (40), and here are shown as a general characterization of the area to demonstrate that the physical and chemical conditions, at this stage of the experiment, are similar between treatments.

2.3 Soil sampling and HMs analysis

In September 2023, a soil sample block measuring 20 cm (width) × 20 cm (length) × 10 cm (thickness) was collected using a cutting blade from the center of each 20 m^2 plot revegetated with perennial grasses in each block. The samples were stratified into two layers (0.00–0.10 m and 0.10–0.20 m). Thus, a total of 24 samples were obtained (four blocks × three treatments × one subsample per treatment × two layers). The soil samples were air-dried, ground, sieved, and homogenized. Pseudo-total concentrations of Zn, Ba, V, and Cr were determined following the EPA Method 3050B recommended by the United States Environmental Protection Agency (48). Sample digestions were performed at the Soil Chemistry Laboratory, Department of Soils, Federal University of Pelotas (Universidade Federal de Pelotas – UFPel), RS State, Brazil. Element concentrations in the extracts were determined at the Chemical Metrology Laboratory (Laboratório de Metrologia Química – LabMeQui), Department of Chemistry, Federal University of Pelotas (UFPel), using a microwave-induced plasma optical emission spectrometer (MIP-OES, model 4200, Agilent Technologies, Melbourne, Australia) equipped with a OneNeb nebulizer. Nitrogen used to sustain the plasma was generated from atmospheric air using a compressor (model MSV12, Schulz, Joinville, SC, Brazil) coupled to a nitrogen generator (model 4107, Agilent Technologies, Melbourne, Australia).

2.3.1 Assurance of quality and quality control of HMs analysis

The credibility of the obtained data was ensured through standardized testing procedures, such as reagent blank analysis, parallel sample testing, establishment of calibration curves, and standard material recovery. All chemical reagents were either analytical grade or of the highest purity. The plastic containers used in the analyses were immersed in 10% HNO_3 (volume ratio) for at least 48 hours, then washed with ultrapure water and dried in an oven (49–51).

In each analytical batch, a reference sample with known and certified concentrations of Zn, Ba, V, and Cr was analyzed. The percent recoveries for the analyzed HMs ranged from 94% to 109%. Blank samples were also included in each analytical batch for quality control purposes and to calculate the method's detection limit (MDL) (50). The MDL was calculated by measuring the concentration of the substance of interest in seven blank samples and by applying Equation 1 (52):

$$MDL = (\bar{x} + t \times s) \times d \quad (1)$$

where: $\bar{x}$ is the average concentration of the substance of interest in seven blank samples, t is the Student's t value at a 0.01 probability level and n-1 degrees of freedom (for n = 7 and $\alpha = 0.01$, t = 3.14), s is the standard deviation of the seven blank samples, and d is the dilution factor used in each method. The calculated values of MDL were 5.3, 2.6, 4.7, and 3.5 mg kg^{-1} for Zn, V, Ba, and Cr, respectively. The recovery rate for the internal sample was 81% ± 12%, which is considered satisfactory to ensure quality control. The internal sample consisted of a matrix spike, prepared by adding known concentrations of the target elements to representative soil samples prior to digestion, in order to assess matrix effects and method performance under the same extraction and analytical conditions applied to the experimental samples. In addition, all digested samples and quality control materials were measured in laboratory triplicates on the MIP-OES instrument to ensure analytical precision.

2.3.2 Risk assessment

The CF, PI, potential ecological risk factor (Er), and RI were used for risk assessment. The classification criteria are presented in Table 3.

The CF is a single-element index that quantifies the degree of soil contamination by comparing the concentration of a given metal to its reference value, indicating the level of enrichment relative to natural conditions. The CF was calculated by dividing the concentration of the HM (Zn, Ba, V, or Cr) in the soil samples by the reference environmental value according to Equation 2 (53):

TABLE 3 Environmental risk assessment classifications for: contamination factor (CF), pollution index (PI), ecological risk (Er) and potential ecological risk index (RI).

Contamination factor (CF)		Pollution index (PI)		Ecological risk (Er)		Potential ecological risk index (RI)	
CF < 1	Low contamination	PI < 1	Low pollution	Er < 40	Low ecological risk	RI < 150	Low ecological risk
1 ≤ CF < 3	Moderate contamination	1 ≤ PI < 2	Moderate pollution	40 ≤ Er < 80	Moderate ecological risk	150 ≤ RI < 300	Moderate ecological risk
3 ≤ CF < 6	Considerable contamination	2 ≤ PI < 3	High pollution	80 ≤ Er < 160	Considerable ecological risk	300 ≤ RI < 600	Considerable ecological risk
CF ≥ 6	Very high contamination	PI ≥ 3	Very high pollution	Er ≥ 160	High to very high ecological risk	RI ≥ 600	Very high ecological risk

$$CF = \frac{\text{Concentration of each HM}}{\text{QRV of each HM}} \quad (2)$$

The Quality Reference Value (QRV) refers to a regulatory environmental reference value that represents the natural (geochemical background) concentration of elements in soils, as established by Brazilian environmental legislation (36). The QRV values are as follows: Ba: 74 mg kg^{-1}, Cr: 25 mg kg^{-1}, Zn: 31 mg kg^{-1}, V: 56 mg kg^{-1} (36, 54). The PI is an integrated index that reflects the overall pollution status of the soil by combining contamination information, providing a synthetic assessment of the intensity of soil pollution. The PI was calculated for each sample considering the average and maximum values of the CF for each HM (Zn, Ba, V, and Cr) in the soil according to Nemerow (55), as in Equation 3:

$$PI = \sqrt{\frac{(CF_{average})^2 + (CF_{maximum})^2}{2}} \quad (3)$$

2.3.3 Ecological risk

The Er of a given contaminant (Zn, Ba, V, and Cr) was calculated according to Keshavarzi and Kumar (56), as in Equation 4:

$$Er = CF \star Ti \quad (4)$$

where: CF is the contamination factor (calculated in equation 2), and Ti is the toxic response factor for a given substance (Cr = V = 2, Zn = Ba=1) (53, 57).

The potential ecological risk index (RI) was developed by Hakanson (53) and can be used to assess the degree of environmental risk caused by a group of HMs present in the soil (58). The RI is calculated as in Equation 5:

$$RI = \Sigma Er = \Sigma(CF \star Ti) \quad (5)$$

where: RI (unitless) is the total potential ecological risk index for all investigated HMs (calculated in equation 4), Er is the single ecological risk index for a specific element (defined in equation 4), and Ti is the toxic response factor for a given substance (Cr = V = 2, Zn = Ba=1) (53, 57). It should be noted that the original RI framework was proposed considering a broader set of contaminants. Therefore, in this study, RI values derived from a reduced number of elements (Zn, V, Cr, and Ba) are interpreted as a relative and site-specific indicator of potential ecological risk, and comparisons with studies using a larger suite of elements should be made with caution.

2.3.3.1 Soil fauna sampling and analysis

In October 2023, a total of 12 square soil monoliths (four replicates x three treatments x one layer) with dimensions of 0.20 m depth were collected for the evaluation of macrofauna organisms according to The Tropical Soil Biology and Fertility method (59). For that, all organisms visible to the naked eye were considered part of the macrofauna (60).

The sampling of mesofauna organisms inhabiting the 0.00–0.10 m soil layer was performed using steel cylinders (8.5 cm in diameter and 10 cm in height). A total of 24 steel cylinders (four replicates x two subsamples x three treatments x one layer) were used. In the laboratory, the Tullgren Extraction Funnel method (61) was applied to extract fauna from the soil cores. For that, the cylinders were carefully placed on sieves with a 2 mm mesh, which were set on top of the funnels. The samples were exposed to 40-watt lamps for 48 hours to induce the organisms to move downwards into a collection cup positioned at the bottom of the funnel. The collection cups contained ethanol (70%) to preserve the organisms until their identification. The sampling of mesofauna inhabiting the litter-soil interface was performed by installing pitfall traps (two per plot) into the holes left after removal of the steel cylinders (62). The traps remained in the field for seven consecutive days. The organisms inhabiting the soil interior and the litter-soil interface were identified in taxonomic groups according to Gallo et al. (63) with the aid of a trinocular stereomicroscope.

The total abundance of the fauna (macro and mesofauna) individuals per taxonomic group was expressed as the number of individuals collected in each treatment per m^2. The number of individuals of each taxon was counted and the various taxa were classified based on the number of individuals as follows: (1) Dominant: > 10% of the total number of individuals captured; (2) Common: 1–10% of the total number of individuals; (3) Rare: 0.1–1% of the total number of individuals; and (4) Extremely rare: < 0.1% of the total number of individuals (64). Additionally, the Shannon-Weiner diversity index (H′), and the Pielou's evenness index (Js) were calculated using the DivEs - Diversity of Species® software (2018-2021, version 4.17) to assess fauna community diversity. The H' and Js indexes were calculated by Equation 6:

$$H' = \sum_{i=1}^{s} pi \, . \log_2(pi) \quad (6)$$

Where: pi = probability of meeting a taxon i and s = total number of taxa found.

The J index indicates the uniformity of fauna individuals, i.e., how individuals in the sample are distributed among the different taxa, calculated by Equation 7:

$$J = \frac{H'}{\log 2(s)} \quad (7)$$

2.3.4 Human health risk assessment

The human health risk models, including carcinogenic and non-carcinogenic risks, developed by the Environmental Protection Agency (65, 66), have been successfully used worldwide. Humans (adults and children) can be exposed to contaminants (e.g., Zn, Ba, V, and Cr) present in the soil through the following main pathways: direct ingestion of soil particles (Equation 8), inhalation of soil particles suspended in the air (Equation 9), and dermal contact with soil particles (Equation 10). The average daily intake (ADI) of chemicals in soils is calculated using the following equations:

$$ADI_{ing} = \left(\frac{C * IngR * EF * ED}{BW * AT}\right) * CF \quad (8)$$

$$ADI_{inh} = \frac{C * InhR * EF * ED}{PEF * BW * AT} \quad (9)$$

$$ADI_{dermal} = \left(\frac{C * SL * SA * ABS * EF * ED}{BW * AT}\right) * CF \quad (10)$$

Where: ADI_{ing} is the average daily intake by direct ingestion; C is the concentration of the HM in soil (mg kg^{-1}); IngR is the ingestion rate (mg day^{-1}) = 100 mg day^{-1} for adults and 200 mg day^{-1} for children (65); ADI_{inh} is the average daily intake by inhalation; InhR is the inhalation rate (m^3 day^{-1} = 7.6 for adults and 20 for children; EF is the exposure frequency = 180 day/year (65); ED is the exposure duration = 24 years for adults and 6 years for children (65); ADI_{dermal} is the average daily intake by dermal contact; SL is the adherence factor = 0.07 mg cm^{-2} for adults and 0.2 mg cm^{-2} for children (65); SA is the exposed area = 5374 cm^2 for adults and 2848 cm^2 for children (65); ABS is the dermal absorption factor = 0.001 for all considered elements (65); BW is the body weight = 70 kg for adults and 20 kg for children (65); and AT is the averaging time, for noncarcinogens = ED × 365 days, and for carcinogens = 365 x 75 (65); CF is the unit conversion factor (1000).

2.3.4.1 Non-carcinogenic risk assessment

The hazard quotient (HQ) is typically employed to assess non-carcinogenic risk. The HQ is obtained as the ratio between the average daily dose and the reference dose (RfD) for a given substance (Supplementary Table 1) according to Equation 11:

$$HQ = \frac{ADI}{RfD} \quad (11)$$

where: RfD is the reference dose for the HM (mg kg^{-1} day^{-1}), which represents the maximum acceptable level of HM that does not pose harmful effects to humans. The human (adults and children) health risk assessment was conducted using non-carcinogenic hazards through the calculation of HQ and HI for three exposure pathways: oral ingestion (ing), inhalation (inh), and dermal contact (dermal).

The global non-carcinogenic risk posed by the various HMs was calculated as the sum of the HQ values for all HMs and expressed as the Hazard Index (HI) according to Equation 12:

$$HI = \Sigma HQi = \Sigma \frac{ADIi}{RfDi} \quad (12)$$

where: HI is the total non-carcinogenic hazard index of the investigated HMs; HQi is the hazard quotient for each HM (Zn, Ba, V and Cr) calculated in equation (9); ADIi is the average daily intake for each HM (Zn, Ba, V and Cr) calculated in equations (8), (9) and (10); and RfD is the reference dose for the HM (mg kg^{-1} day^{-1}) (Supplementary Table 1). The risk is considered low or insignificant if HI < 1, and a non-carcinogenic risk exists if HI > 1 (67).

2.3.4.2 Carcinogenic Risk Assessment

The carcinogenic risk is defined as the probability of a human being developing cancer because of exposure to carcinogenic hazards. The carcinogenic risk (associated with Cr levels) (CR) for a human was computed according to USEPA (68) according to Equation 13:

$$CR = ADI * SF \quad (13)$$

where: CR is the carcinogenic risk of specific HMs (calculated only for Cr because among the investigated HMs Cr was the only one found in concentrations posing carcinogenic risk); SF is the carcinogenic slope factor for the exposure pathway of the HM (mg kg^{-1} day^{-1}) for Cr the values considered were 8.50E-03 for ingestion and 4.20E + 01 for inhalation risk. If CR is <1.0E-06, the risk is low or insignificant; if CR is between 1.0E-06 and 1.0E-04, the risk is considered acceptable; if CR >1.0E-04, the carcinogenic risk is high (67).

2.4 Data analysis

One-way ANOVA was performed to assess the effect of treatments (grass species) on the concentration of HMs in each soil layer, after verifying the assumptions of normality and homogeneity of variances. When these assumptions were not met (only Cr and Ba at 0.00–0.10 m layer), the Kruskal–Wallis' test was applied to detect treatment effects. The ANOVA and the Kruskal–Wallis' test were performed in SIGMAPLOT 12.3 revealed no significant treatment effect on the concentration of HMs, regardless of soil layer. Therefore, *post-hoc* tests for comparison of treatment averages were unnecessary.

Principal component analysis (PCA) was used to explore the influence of the different grasses used for minesoil restoration and the concentration of HMs on soil fauna communities. For PCA analysis, only fauna communities that represented at least 2% of the sampled fauna (Acari, Araneae, Entomobryomorpha, Blattaria, Coleoptera, Diptera, Hymenoptera, Earthworm), and fauna individuals in adult form were considered. The soil layer considered for PCA analysis was 0.00–0.10 m layer to provide an overview of the impact of HMs on fauna inhabiting the topsoil. For PCA, only attributes with significant correlation (|r| ≥ 0.65) and eigenvalues greater than 1 were used, which allowed excluding variables with low influence on the total variation. The PCA analysis was performed using PAST 4.03 statistical software (PAleontological STatistics) (69).

3 Results and discussion

3.1 Content of HMs in soil

Overall, there were no significant treatment effects on the levels of HMs in the soil, regardless of the soil layer (Table 4). When analyzing the average contents of the four HMs in the soil, it is verified that only the contents of Zn (both layers) remained below

TABLE 4 **Quality reference value (QRV) and summary statistics of heavy metals (HMs) content (mg kg^{-1}) of a minesoil restored for 20 years with perennial grasses (*Cynodon dactylon*, *Urochloa brizantha* and *Hemarthria altissima*).**

HMs	QRV (mg kg^{-1})		*Cynodon dactylon*	*Urochloa brizantha*	*Hemarthria altissima*
			----0.00–0.10 m layer---		
Zn		Average	25.0 [ns*]	23.9	24.0
		Maximum	31.5	66.9	29.5
	31.0 [a]	Minimum	20.5	91.0	17.5
		SD	4.0	27.0	4.9
		CV (%)	16.1	24.6	20.6
V		Average	93.1 [ns*]	89.6	110.6
		Maximum	103.6	126.0	166.6
	56.0 [a]	Minimum	82.6	30.1	82.6
		SD	7.8	22.8	38.3
		CV (%)	8.4	40.6	34.7
Ba		Average	101.5 [ns**]	77.0	122.5
		Maximum	105.0	23.1	189.0
	74 [b]	Minimum	91.0	0.8	91.0
		SD	6.1	20.9	45.2
		CV (%)	6.0	23.6	36.9
Cr		Average	28.4 [ns**]	27.0	36.2
		Maximum	37.1	3.2	51.1
	25 [a]	Minimum	23.1	31.3	30.1
		SD	5.8	15.9	10.1
		CV (%)	20.5	13.7	27.8
HMs			---0.10–0.20 m layer ---		
Zn		Average	16.8 [ns*]	21.6	25.1
		Maximum	28.5	63.2	38.5
	31.0 [a]	Minimum	10.5	90.3	17.5
		SD	8.5	29.4	9.3
		CV (%)	50.7	31.5	37.1
V		Average	91.4 [ns*]	82.6	89.6
		Maximum	103.6	105.0	103.6
	56.0 [a]	Minimum	82.6	31.4	47.6
		SD	8.8	10.5	28.0
		CV (%)	9.6	47.6	31.3
Ba		Average	126.0 [ns*]	79.0	112.0
		Maximum	147.0	25.0	147.0
	74 [b]	Minimum	105.0	8.8	91.0
		SD	20.6	14.5	24.2
		CV (%)	16.4	12.4	21.7
Cr		Average	25.0 [ns*]	30.0	28.4
		Maximum	30.1	40.9	30.1
	25 [a]	Minimum	23.1	23.0	23.1
		SD	3.5	13.8	3.5
		CV (%)	14.1	10.2	12.3

SD, standard deviation of the mean; CV (%), coefficient of variation. [a]QRV for soils in Rio Grande do Sul State, Brazil (36). [b]Quality reference values (QRV) for soils in the State of São Paulo, Brazil (54). ns: not significant according to ANOVA* and Kruskal–Wallis** test among perennial grasses.

the quality reference value (QRF) of 31 mg kg^{-1}, valid for the experimental location (36). Conversely, the contents of V, Ba and Cr found in the soil were above their respective QRF (Table 4). Likely, the enrichment of the soil with V, Ba and Cr reflects the extraction and combustion activities typical of the coal mining sector (70). The proximity (6 km) of the coal power plant to the experiment may have facilitated the deposition of contaminated dust on the studied soil, as similarly observed by (71, 72). Also, the elevated contents of V, Ba and Cr may result from the utilization of mining tailings for the topographic reconstitution of this mined land and from the presence of overburden layers within the 0.00–0.30 m layer in the studied soil as reported by Stumpf et al. (45) and Burgueño et al. (73).

The average content of V observed at the 0.00–0.10 m layer in *H. altissima*, *C. dactylon* and *U. brizantha* treatments was 2.0-, 1.7- and 1.6-fold higher, respectively, than the QRV (56 mg kg^{-1}) (Table 4). The average content of V observed at the 0.10–0.20 m layer in *H. altissima*, *C. dactylon* and *U. brizantha* treatments was 89.6, 91.4 and 82.6 mg kg^{-1}, respectively. These values are considerably lower compared to those found at the 0.00–0.10 m layer, especially in *H. altissima* where the average V decreased by 19% at the lower compared to the upper layer. However, these average V values were still 1.5- to 1.6-fold higher than the QRV (Table 4). The fate of these HMs in the studied environment may be studied in detail in future studies.

The high contents of V observed in this study may reflect typically high levels of V found in mineral coals, which is often close to 100 mg kg^{-1} (74, 75). For instance, the enrichment of soils with V near coal-fired power plants due to the deposition of dust from coal excavation and ash from coal combustion was reported by Xiao et al. (76). After entering the soil, V can bind to organic compounds and/or adsorb on the surface of clay minerals, mainly Fe oxides. This chemical affinity occurs because at soil pH around 5.5, as observed in our study (Table 2), the surface of Fe oxides is predominantly charged positively due to its elevated point of zero charge (>7). Also, at a pH range of 5.5 to 6.0, the major chemical form of V is VO_3^- (77). Thus, VO_3^- binds to Fe oxides via ligand exchange and forms an inner-sphere complex, resulting in V immobilization and persistence in the soil.

The average Ba content at the 0.00–0.10 m layer in *H. altissima*, *C. dactylon* and *U. brizantha* treatments was 1.7, 1.4 and 1.04-fold higher, respectively, than the QRV of 74 mg kg^{-1} (54) (Table 4). At the 0.10–0.20 m layer the average Ba contents were 1.7-, 1.5- and 1.05-fold higher, respectively, compared to the QRV (Table 4). Mineral coal often contains high concentrations of Ba, 150 mg kg^{-1} as the global average (78). In southern Brazil, the Ba content in mineral coal ranges from 70 to 1375 mg kg^{-1}, with an average of 291 mg kg^{-1} (74). Likely, this partially explains the elevated Ba content found in the studied minesoil, even after 20 years of restoration. Once in the soil, Ba can be strongly retained by clay minerals and oxides, and preferentially binds to Mn (hydr)oxides rather than to Fe (hydr)oxides (79). The chemical affinity of Ba for Mn oxides, rather than for Fe or Al oxides, can be attributed to the lower point of zero charge of Mn minerals and oxides, which range from 1.5 in birnessite to 6.0 in hausmannite (71, 80). Thus, the pH of the studied soil (5.0 to 6.0, Table 2) confers a predominant negative charge in the surface of these minerals, facilitating the adsorption of Ba^{2+}.

The highest average content of Cr at the 0.00–0.10 m layer was observed in the *H. altissima* treatment (36.2 mg kg^{-1}), followed by *C. dactylon* (28.4 mg kg^{-1}) and *U. brizantha* (27.0 mg kg^{-1}) (Table 4). These values are 1.45-, 1.14- and 1.08-fold higher than the QRV for Cr (25 mg kg^{-1}) valid for the study location (36). The average soil Cr content at the 0.10–0.20 m layer decreased by 12% and 22% under *C. dactylon* and *H. altissima*, respectively, compared to the 0.00–0.10 m layer. Conversely, for the *U. brizantha* treatment, the average Cr content at the 0.10–0.20 m layer increased by 11% compared to the 0.00–0.10 m layer (Table 4). At the 0.10–0.20 m layer, the average Cr content in *U. brizantha* and *H. altissima* were 1.20 and 1.14 fold higher than the QRV for Cr, whereas in *C. dactylon* the Cr content did not differ from the QRV (Table 4). Chromium is one of the main HMs found in mineral coal (81). In southern Brazil, Cr contents ranging from 48 to 56 mg kg^{-1} have been reported in coal mining waste (82). As previously mentioned, Cr and other HMs are released during the combustion of coal. Chromium is a metallic element with variable valence states and typically occurs as Cr(III) and Cr(VI) in the environment (83, 84). Manganese oxides present in soils oxidize Cr(III) to Cr(VI), which is highly mobile in soil (85, 86) usually resulting in a decline of Cr content in soil over time. However, this phenomenon was likely minimized in the studied soil, as most of the Cr present was probably in the form of Cr(III). This is because Cr(III) precipitates at pH values above 5.5 (Table 2). Therefore, Cr(III) compounds may remain stable in the soil under these conditions. This stability may explain the high concentrations of Cr ≥ QRV (25 mg kg^{-1}) detected in the studied soil even after 20 years of restoration.

The persistence of HMs in soil has been demonstrated at the abandoned Tab-Simco coal mine in Illinois (USA), where high contents of Fe, Zn, Ni, Cr, Cu, Pb, and Cd (41, 419, 175, 152, 148, 145, and 4 mg kg^{-1}, respectively) were observed in the soil even after 40 years of mine's closure (87). These findings agree with (88), who found elevated contents of Cd, Cr, Zn, Ni and Pb, as well as elevated geoaccumulation index (Igeo) values for Cr (classes 1 to 3) and Cd (classes 2 to 5) in the post-coal mine soil of Xinzhuangzi (China) used as farmland.

Bearing in mind that the interpretation of so-called pseudo-total concentration of HMs alone is limited (89) as their mobility, bioavailability and ecotoxicity may be affected by soil properties and processes (90, 91), a series of HMs risk assessment indexes is presented below.

3.2 Risk assessments

3.2.1 Environmental risk: contamination factor and pollution index

Overall, only the CF of Zn was classified as "low contamination" (CF < 1), regardless of the treatment and soil layer (Figure 2). The CF of V, Ba and Cr was classified as "moderate contamination" (1 ≤ CF > 3), regardless of the treatment and soil layer (Figure 2). No changes in CF classification were detected between the 0.00–0.10 m

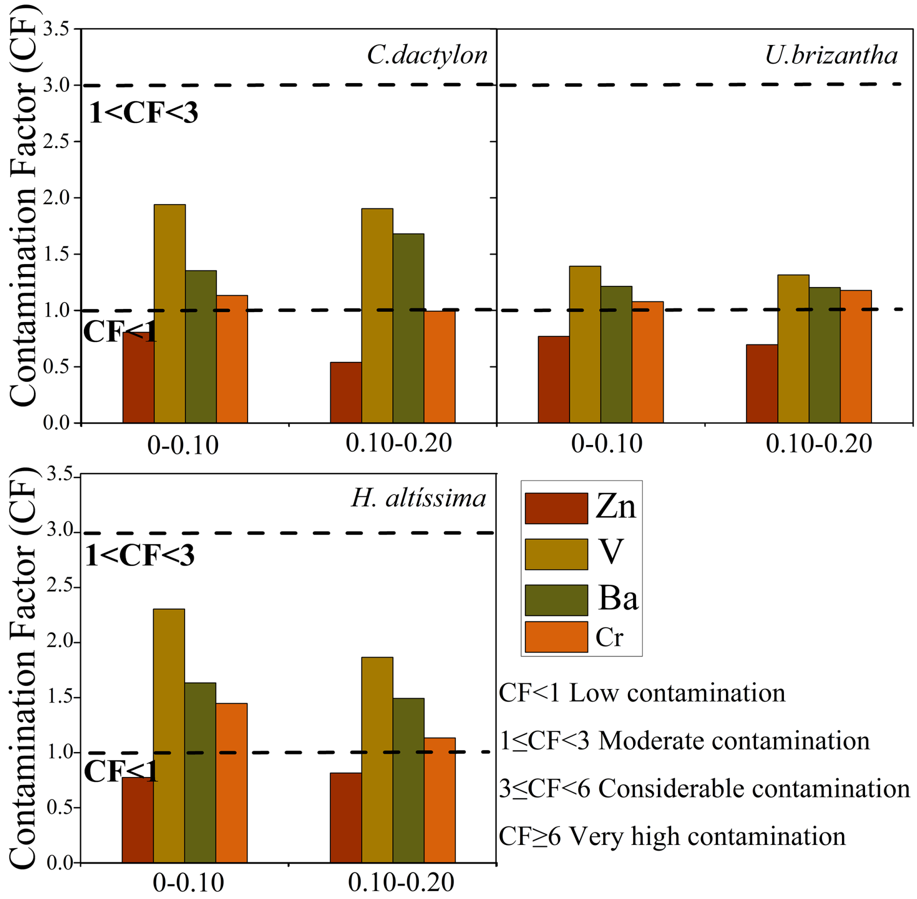

FIGURE 2
Contamination fator (CF) for Zn, V, Ba and Cr at 0.00–0.10 m and 0.10–0.20 m layer of a minesoil restored for 20 years with perennial grasses (*Cynodon dactylon*, *Urochloa brizantha* and *Hemarthria altissima*).

and 0.10–0.20 m layers for any HMs, indicating that soil depth did not influence CF-based contamination patterns. Even though the CF for V, Ba and Cr remained within the same CF class (moderate contamination) across the treatments and soil layers (Figure 2), V consistently showed higher CF values compared to the other HMs, regardless of treatment or soil layer (Figure 2). When comparing the treatments, it is noticeable that the CF values for V, Ba and Cr tended to be lower in *U. brizantha*, except for Cr at the 0.10–0.20 m layer. On the other hand, the CF values for V, Ba and Cr tended to be higher in *H. altissima*, especially at the 0.00–0.10 m layer (Figure 2). Although slight numerical differences between soil layers were observed for some HMs, these variations did not result in changes in CF classification.

The PI was used to assess the magnitude of HM contamination in the studied soil despite its long-term restoration with perennial grasses. In fact, the PI values revealed that the soil was at least slightly or severely polluted depending on the HM, treatment, and soil layer (Figure 3). Notably, PI values indicative of unpolluted soils were absent (Figure 3). The soil restored with *C. dactylon* and *U. brizantha* exhibited PI values close to or below 2, regardless of HM and soil layer, indicating slight or modest pollution levels, as similarly observed for *H. altissima* at the 0.10–0.20 m layer (Figure 3). Notably, in the 0.00–0.10 m layer under the *H. altissima* treatment, the PI for V (3.22) classified the soil as severely polluted, and the PI for Ba (2.17) indicated heavy pollution (Figure 3). Overall, these findings indicate that the grass species used for minesoil restoration strongly influences the level of soil contamination by HMs, whereas soil depth plays a secondary role. In view of the potential toxicity and high persistence of these HMs in soil, soils polluted with such elements pose an environmental problem that threatens animal, plant, and human health (29). In plants, the toxicity of Ba, V, and Cr can disrupt morphological, biochemical, and ultrastructural functions, as well as disturb their nutritional balance. However, *C. dactylon*, *U. brizantha*, and *H. altissima* seem to at least tolerate these HMs as they have satisfactorily grown for about 20 years in the study area. The grasses can be visualized in Leal et al. (92).

At the 20-year restoration scale, differences in soil HMs concentrations among perennial grass species are likely related to long-term, plant-mediated changes in soil properties, since biomass harvesting was not performed. Species-specific differences in root architecture, root turnover (45), and rhizosphere activity may have progressively altered soil pH and metal–soil interactions (98, 99), thereby influencing metal speciation, mobility, and redistribution within the soil profile (99). Over this time frame, part of the metals may also have been displaced from the sampled layers through leaching or volatilization, while another fraction may have become increasingly adsorbed or incorporated into mineral structures (77,

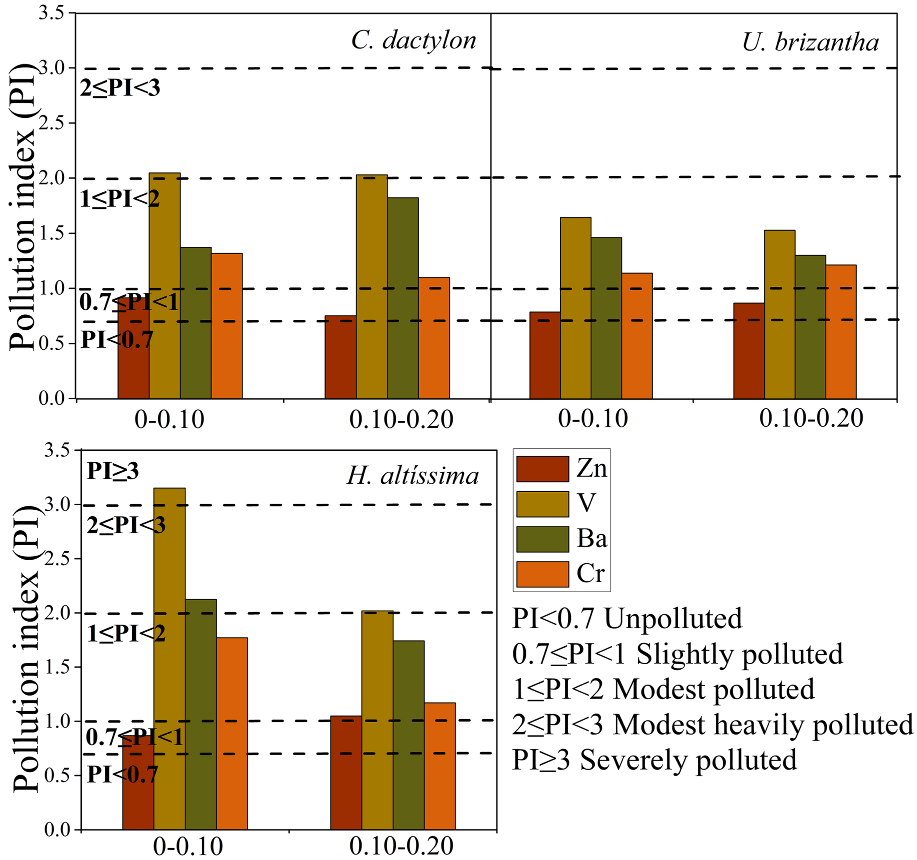

FIGURE 3
Pollution index (PI) for Zn, V, Ba and Cr at 0.00–0.10 m and 0.10–0.20 m layer of a minesoil restored for 20 years with perennial grasses (*Cynodon dactylon*, *Urochloa brizantha* and *Hemarthria altissima*).

79, 80). These long-term, species-dependent soil processes may partially account for the contrasting contamination indices observed among the perennial grasses evaluated in this study.

In this context, the different abilities of the perennial grasses used in this study to reduce contamination indices of the soil with HMs may be associated with the fact that, in addition to being tolerant, they may act as phytostabilizers, phytovolatilizers, phytodegraders, phytostimulators, or phytoextractors of HMs. In particular, this is evidenced by the overall lower CF and PI in the soil with *U. brizantha* compared to *C. dactylon* and *H. altissima* (Figures 2, 3). Plants that thrive in HM-contaminated soils typically employ two main survival strategies: avoidance or tolerance (93). Avoidant species prevent HMs from entering the protoplast, whereas tolerant species neutralize or remove HMs from metabolically sensitive areas (94). In fact, the high potential of *U. brizantha* for phytoremediation purposes has been demonstrated in different studies and attributed to its phytoextraction characteristics, such as a high growth rate, biomass production, root development, and the ability to tolerate and accumulate HMs such as V, Ba, and Cr (95, 96). This is in line with Stumpf et al. (45), who found greater root density in the soil with *U. brizantha* compared to *C. dactylon* and *H. altissima* after 8.6 years of restoration in the same experimental site. It is known that *U. brizantha* employs a tolerance-based survival strategy, via phytolith production (70, 96, 97). Phytoliths are structures composed of amorphous silica that precipitate alongside HMs within the cell walls of roots, thereby neutralizing the HMs and consequently reducing their toxicity (98, 99). The higher concentration and accumulation of HMs in roots compared to shoots in grasses have been reported by Ullah et al. (100). Similarly, Sundaramoorthy et al. (101) reported greater accumulation of Cr (251.6–275.5 mg kg^{-1}) in roots compared to shoots of grass species (*C. kylinga* and *C. rotundus*) cultivated in Cr-contaminated soils.

In a lower extent, *C. dactylon* also demonstrated potential for reducing CF and PI values in the soil if compared to *H. altissima*, maintaining the soil within a range of moderate pollution by V, Ba, and Cr (Figures 2, 3). The literature suggests that *C. dactylon* is a promising species for phytostabilization compared to shrubs and trees, owing to its high growth rate, adaptability to abiotic stresses and dense soil coverage (17, 102). One advantage of dense soil coverage is the reduction of windborne particle movement and the associated transport of HMs into the surrounding environment (103). Consequently, this can reduce the risks to human health associated with the inhalation or ingestion of contaminated soil particles (104).

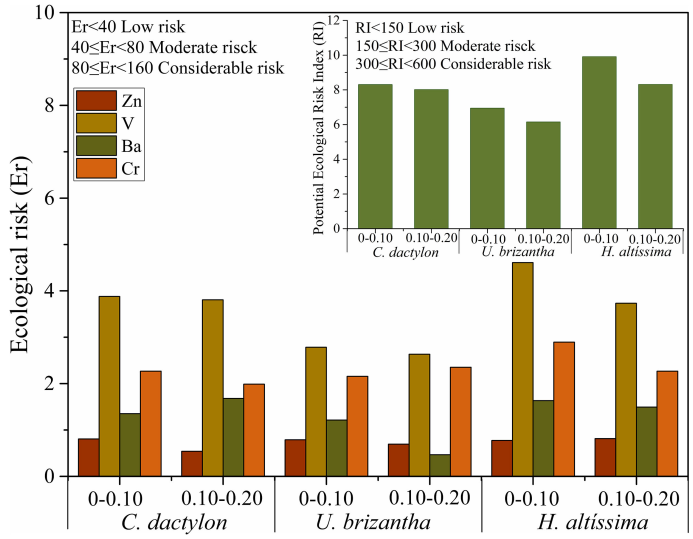

FIGURE 4
Ecological risk (Er) for Zn, V, Ba and Cr and their grouped potential ecological risk index (RI) at 0.00–0.10 m and 0.10–0.20 m layer of a minesoil restored for 20 years with perennial grasses (*Cynodon dactylon*, *Urochloa brizantha* and *Hemarthria altissima*).

3.2.2 Ecological risk assessment

3.2.2.1 Potential ecological risk factor of individual HMs and potential ecological risk index

The concentrations of HMs observed in the soil, regardless of treatment and soil layer, were insufficient to represent a significant Er (Figure 4). All Er values were below 5 and therefore indicate low ecological risk (Figure 4). Comparing HMs, it is noteworthy that the highest Er values occurred for V, regardless of treatment and soil layer, and were particularly high in *H. altissima* (Figure 4). Furthermore, it is noteworthy that although the CF and PI values for Cr were lower than those for Ba, its Er was higher (Figure 4). This pattern was consistent across both soil layers, suggesting that depth did not modify the relative contribution of Cr to ecological risk. This is attributed to the potential toxicity of Cr to the ecosystem even in low concentrations. In fact, Cr has been classified as carcinogenic to humans by the International Agency for Research on Cancer (105). This is associated with the fact that Cr can accumulate into ecosystems by building up in organisms such as bacteria, plants, and aquatic life, eventually biomagnifying through the food chain and posing a threat to human health (106). According to Stanley et al. (107), prolonged exposure to Cr can adversely affect human reproduction and has been linked to lung cancer, adenocarcinoma, squamous cell carcinoma, and other diseases.

Although the RI was originally proposed based on a broader suite of contaminants, the index is widely applied in studies focusing on a reduced number of elements as a screening and comparative tool for site-specific ecological risk assessment. In this context, the RI values obtained in this study reflect the cumulative contribution of Zn, V, Cr, and Ba and should be interpreted as a relative indicator rather than an absolute measure of ecological risk. Consequently, comparisons with RI values reported in studies that include a larger set of contaminants should be made with caution.

In this study, the RI values remained below 10, regardless of treatment or soil layer, and were therefore classified as low risk (RI < 150) (Figure 4). The low Er and RI values suggest that plant-mediated processes, particularly root exudation, play an important role in modulating soil physicochemical conditions by altering metal speciation and bioavailability, while simultaneously stimulating microbial activity in the rhizosphere, thereby reducing the environmental hazard posed by HMs (108).

In this sense, while the RI provides an integrative and site-specific overview of cumulative ecological risk, the use of Er allows for more robust numerical comparisons among studies, as it directly reflects the potential ecological risk associated with each HM independently. Because Er is not influenced by the number of elements included in the assessment, it represents a more consistent metric for comparing the relative ecological risk of individual metals across different sites, soil layers, and management conditions. Therefore, the consistently low Er values observed in this study confirm the limited ecological risk posed by Zn, V, Cr, and Ba in the investigated soils, while enabling meaningful comparison with similar studies focused on individual contaminants.

3.2.2.2 Influence of HMs concentration on soil fauna communities

Twenty years after minesoil restoration, a total of 6,098 soil fauna individuals were counted in the investigated soil, distributed across five distinct classes. Among these classes, 14 macrofauna groups were identified, including one dominant taxon (Hymenoptera), nine common taxa (Araneae, Carabiform larvae, Coleoptera, Diplopoda, Diptera, Scarabaeiform larvae, Exarada pupae, Thysanoptera, and Earthworms), and four rare taxa (Curculioniform larvae, Dermaptera, Elateriform larvae, Orthoptera). Also, six mesofauna groups were identified, including one dominant taxon (Acari), three common taxa (Entognatha from the orders Entomobryomorpha and

TABLE 5 Number of individuals, relative dominance, diversity index of Shannon-Wierner (H') and evennes index of Pelou (J') for soil fauna found in a minesoil after 20 years of restoration with *Cynodon dactylon*, *Urochloa brizantha* e *Hemarthria altissima*.

Class	Group	Size	*H. altissima*	*U. brizantha*	*C. dactylon*	Dominance
				∑ individuals m^{-2}		
Arachnida	Acari	Meso	485	890	687	33.8%***
	Araneae	Macro	132	122	167	6.9%**
Collembola	Entomobryomorpha	Meso	115	185	176	7.8%**
	Poduromorpha	Meso	0	0	9	0.1%*
	Symphypleona	Meso	0	53	26	1.3%**
Insecta	Blattodea	Meso	0	9	123	2.2%**
	Carabiform Larvae	Macro	0	75	0	1.2%**
	Coleoptera	Macro	62	76	115	4.1%**
	Curculioniform Larvae	Macro	0	0	50	0.8%*
	Dermaptera	Macro	0	25	0	0.4%*
	Diptera	Macro	106	113	53	4.5%**
	Elateriform Larvae	Macro	25	0	0	0.4%*
	Scarabaeiform Larvae	Macro	250	50	150	7.4%**
	Exarate Pupae	Macro	50	125	50	3.7%**
	Hymenoptera	Macro	229	493	357	17.7%***
	Orthoptera	Macro	0	9	0	0.1%*
	Thysanoptera	Macro	34	9	62	1.7%**
Myriapoda	Diplopoda	Macro	0	75	0	1.2%**
Clitellata	Earthworm	Macro	200	0	50	4.1%**
	Enchytraeidae	Meso	26	0	0	0.4%*
	Individual	Macro	1088	1172	1054	
		Meso	626	1137	1021	
	Group	Macro	9	11	9	
		Meso	3	4	5	
	H' index		2.06	1.98	1.31	
	J index		0.69	0.66	0.44	

[1]Degree of dominance: ***Dominant group (>10%); **Commun group (1–10%); *Rare group (0.1–1%).

Symphypleona, and Blattodea), and two rare taxa (Entognatha from the order Poduromorpha and Enchytraeidae) (Table 5).

The outstanding lower content of HMs, CF, PI, Er, and RI values observed in *U. brizantha* likely contributed to the higher number of mesofauna and macrofauna individuals (2,309) in this treatment compared to *C. dactylon* (2,075) and *H. altissima* (1,714 organisms) (Table 5). This is in line with (109), who observed that the total number of organisms and the total taxa number of soil fauna organisms were higher in areas where the content of HMs was lower. Nevertheless, this did not result in a higher fauna diversity index in *U. brizantha* (H'= 1.98), compared to *H. altissima* (H' = 2.06). This is likely due to the greater dominance of the Acari and Insecta classes (group Hymenoptera) in *U. brizantha* treatment, which was 30% and 84% higher, compared to the dominance in *C. dactylon*, and 38% and 115% higher compared to the dominance in *H. altissima* (Table 5), respectively.

During the realization of this study, earthworms were observed for the first time in tis minesoil since the start of the experiment in 2003. However, earthworms only occurred in *H. altissima* and *C. dactylon* treatments (Table 5). In the PCA biplot, the eigenvector of earthworms was ordinated along component 1, which explained 27.15% of the variation in the dataset, and within the same plot quadrant as soil pH and even more closely associated with Zn, V, Ba and Cr contents (Figure 5). Altogether, these data reveal that the number of earthworms (Clitellata group) correlated positively with Cr, V, Zn and Ba content, suggesting that these organisms tolerated the content of HMs found in this soil. This is coherent with the low Er and RI of HMs (both classified as low) found across all treatments and soil layers (Figure 4). For instance, Van Vliet et al. (110) reported that different species of earthworms can accumulate HMs as As, Cr, Cd, Pb, Cu and Zn, allowing them to survive in soils with even high levels of contamination at varying soil depths. The ordination of pH eigenvector within the same quadrant as the eigenvectors of HMs in the PCA biplot indicates that the range of pH values observed in this minesoil favors the persistence of HMs, as discussed earlier, especially if *C. dactylon* is cultivated (Figure 5).

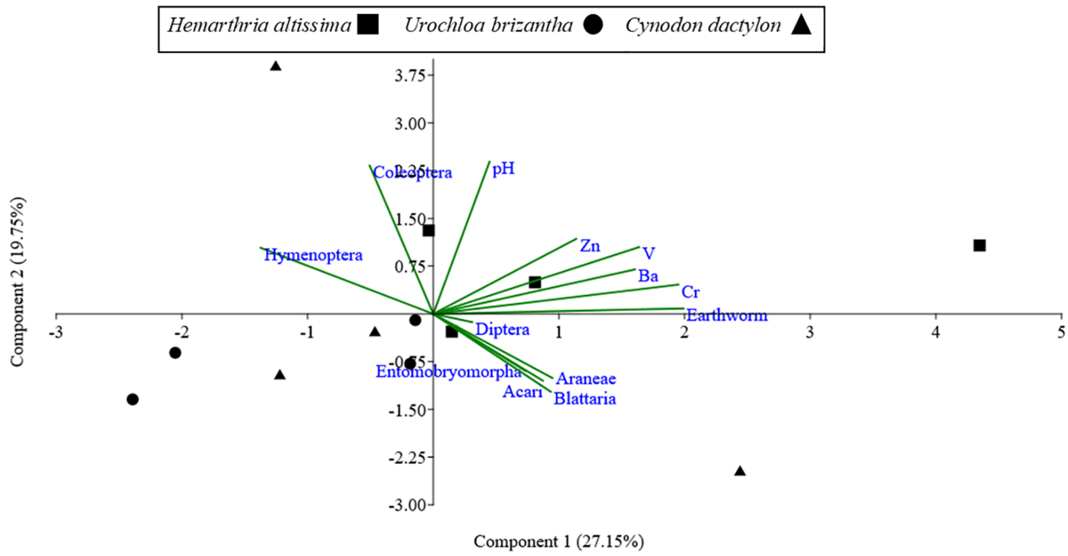

FIGURE 5
Principal component analysis biplot with eigenvectors pointing towards higher values of HMs content, number of fauna individuals and pH in a minesoil restored for 20 years with perennial grasses.

Component 2 of PCA explained 19.75% of the variation in the dataset and clearly separated the dominant fauna groups (Acari e Hymenoptera) and the HMs content in different quadrants in the biplot (Figure 5). These findings suggest the intolerance of Hymenoptera (i.e., ants) to the content of HMs found in this soil. Similar results were observed by Khan et al. (94) for certain ant species in a gradient of soil pollution with Fe, Zn, Mn, Pb and Cu across coal mine spoils of 2, 8 and 12 years old. Regarding Acari communities, future studies may include the division of Acari individuals between decomposers and predators, which may respond differently to HM levels (21, 111), to elucidate the relationship between Acari and HMs content found in this study. Noteworthily, *U. brizantha* was the only treatment where its four replicates were ordinated in the opposite quadrant away from the eigenvectors of HMs, but also in a different quadrant than the eigenvectors of soil fauna (Figure 5). Together, these observations show the role of *U. brizantha* to reduce the content of HMs in the minesoil, without necessarily favoring fauna diversity.

At this point, it is important to highlight that in previous studies conducted in this same area, the minesoil under *U. brizantha* revegetation consistently showed better performance of this treatment to improve soil physical attributes (37, 40, 112). These studies have regarded *U. brizantha* as a pioneer species in the rehabilitation of minesoils at the Candiota Mine, which aligns with the observed reduction in the content of HMs. However, due to the low faunal diversity observed in this treatment, top-down regulation appears to remain weak. This is particularly relevant given that soil microarthropods are known to be efficient recolonizers of Technosols during the early stages of recovery (113, 114). Therefore, regardless of the treatment's effectiveness in improving the soil's physicochemical properties, the low trophic richness observed suggests that recovery is restricted to the soil surface and does not extend to the broader edaphic community. Despite the continuous input of organic matter over 20 years of restoration, the minesoil under *U. brizantha* revegetation does not seem to favor the return of soil fauna –considering their mobility and seasonality– resulting in limited top-down control.

Although the Er and RI found for Zn, V, Ba, and Cr in the present study are classified as "low" (Figure 4), these results provide the first baseline for this field experiment, allowing continuous monitor the development of soil fauna communities' structure in response to these HMs to design optimal restoration strategies (109, 115).

3.2.3 Human health risk assessment

The human health risk assessment was conducted to test if after 20 years of restoration, the studied site could be used as a recreational area for the local community considering that humans may be exposed to contamination by HMs present in the soil through inhalation, dermal contact, or ingestion (116, 117). Another key point is that the experimental area is located near the boundaries of the active mine and in close proximity to urban settlements situated approximately 900 m away. These residential areas include both adults and children, making the assessment of potential human health risks particularly relevant, especially given the potential chronic exposure through soil particle ingestion or inhalation. An essential element for the human body is considered deficient when its concentration falls below the optimal range, while adequacy is attained when it is within this range. Toxicity arises when the concentration of the element exceeds the ideal threshold (116, 118). The human health risk assessment was conducted using non-carcinogenic hazards through the calculation of HQ and HI for three exposure pathways: oral ingestion (ing), inhalation (inh), and dermal contact (dermal) for both adults and children (Tables 6, 7).

The HQing values for Zn remained within the range of 5.93E-05 to 3.93E-05 for adults and 4.26E-04 to 2.82E-04 for children, regardless of treatment and soil layer (Table 6). The highest HQing value of 1E-02 for adults and 8E-02 for children was observed for V in *H. altissima* treatment at the 0.00–0.10 m layer

TABLE 6 Hazard quotient by ingestion (HQing), inhalation (HQinh) and dermal contact (HQdermal) for HMs (Zn, Ba, V and Cr) for adults and children found at the 0.00–0.10 m and 0.10–0.20 m layer of a minesoil restored for 20 years with perennial grasses (*Cynodon dactylon*, *Urochloa brizantha* and *Hemarthria altissima*).

Grass	Layer (m)	Adults				Childrem			
		Zn	V	Ba	Cr	Zn	V	Ba	Cr
		HQing				HQing			
C. dactylon	0.00–0.10	6E-05	9E-03	1E-03	2E-03	4E-04	7E-02	7E-03	4E-03
C. dactylon	0.10–0.20	4E-05	9E-03	1E-03	2E-03	3E-04	7E-02	9E-03	3E-03
H. altissima	0.00–0.10	6E-05	1E-02	1E-03	3E-03	4E-04	8E-02	9E-03	5E-03
H. altissima	0.10–0.20	6E-05	9E-03	1E-03	2E-03	4E-04	6E-02	8E-03	4E-03
U. brizantha	0.00–0.10	6E-05	7E-03	9E-04	2E-03	4E-04	5E-02	7E-03	4E-03
U. brizantha	0.10–0.20	5E-05	6E-03	9E-04	2E-03	4E-04	5E-02	7E-03	4E-03
		HQinh				HQinh			
C. dactylon	0.00–0.10	9E-09	1E-06	7E-05	3E-05	2E-05	3E-03	1E-01	2E-01
C. dactylon	0.10–0.20	6E-09	1E-06	9E-05	3E-05	1E-05	3E-03	2E-01	2E-01
H. altissima	0.00–0.10	8E-09	2E-06	9E-05	4E-05	2E-05	3E-03	2E-01	2E-01
H. altissima	0.10–0.20	9E-09	1E-06	8E-05	3E-05	2E-05	2E-03	2E-01	2E-01
U. brizantha	0.00–0.10	8E-09	1E-06	7E-05	3E-05	2E-05	2E-03	1E-01	2E-01
U. brizantha	0.10–0.20	7E-09	9E-07	7E-05	3E-05	1E-05	2E-03	1E-01	2E-01
		HQdermal				HQdermal			
C. dactylon	0.00–0.10	1E-06	4E-03	5E-05	4E-04	6E-06	2E-02	3E-04	5E-04
C. dactylon	0.10–0.20	7E-07	3E-03	7E-05	4E-04	4E-06	2E-02	4E-04	5E-04
H. altissima	0.00–0.10	1E-06	4E-03	7E-05	5E-04	6E-06	2E-02	4E-04	7E-04
H. altissima	0.10–0.20	1E-06	3E-03	6E-05	4E-04	6E-06	2E-02	3E-04	5E-04
U. brizantha	0.00–0.10	1E-06	3E-03	5E-05	4E-04	6E-06	1E-02	3E-04	5E-04
U. brizantha	0.10–0.20	1E-06	2E-03	5E-05	4E-04	5E-06	1E-02	3E-04	6E-04

(Table 6). According to USEPA (119), V is classified under two pollutant groups: "heavy metals" and "inorganic pollutants". Exposure to V can cause symptoms such as coughing, upper respiratory tract irritation, gastrointestinal disorders, or conjunctivitis (120).

The highest HQ values of 1E-01 and 2E-01 were observed for Ba and Cr, respectively, for children through the inhalation exposure pathway (HQinh), regardless of treatment and soil layer (Table 6). The HQinh associated with Cr is attributed to its volatilization potential, as Cr (VI) is highly volatile in soil, both in acidic and alkaline environments (85, 121). In addition to this direct soil emission, HMs such as Ba and Cr can be volatilized through absorption by plant roots, followed by their conversion to gaseous state and release into the atmosphere, a process known as

TABLE 7 Non-carcinogenic Hazard Index of HMs (ZN, V, and Ba) by ingestion (HIing), inhalation (HIinh) and dermal contact (HIdermal), and carcinogenic risk index by ingestion (CRing) and inhalation (CRinh) for chromium for adults and children exposed to the minesoil (0.00–0.10 m and 0.10–0.20 m layer) after 20 years of restoration with perennial grasses.

Grass	Layer (m)	Non-Carcinogenic					
		Adults	Children	Adults	Children	Adults	Children
		HIing		HIinh		HIdermal	
C. dactylon	0.00–0.10	1.05E-02	7.5E-02	7.5E-05	1.4E-01	3.6E-03	1.9E-02
C. dactylon	0.10–0.20	1.1E-02	7.5E-02	9.3E-05	1.7E-01	3.5E-03	1.9E-02
H. altissima	0.00–0.10	1.2E-02	8.9E-02	9.0E-05	1.7E-01	4.3E-03	2.3E-02
H. altissima	0.10–0.20	1.0E-02	7.3E-02	8.2E-05	1.5E-01	3.5E-03	1.9E-02
U. brizantha	0.00–0.10	7.7E-03	5.5E-02	6.7E-05	1.2E-01	2.6E-03	1.4E-02
U. brizantha	0.10–0.20	7.3E-03	5.3E-02	6.6E-05	1.2E-01	2.4E-03	1.3E-02

(Continued)

TABLE 7 Continued

Grass	Layer (m)	Carcinogenic[a] (chromium)					
		Adults	Children	Adults	Children		
		CRing		CRinh			
C. dactylon	0.00–0.10	5.4E-08	9.8E-08	3.9E-08	2.3E-04		
C. dactylon	0.10–0.20	4.8E-08	8.5E-08	3.5E-08	2.0E-04		
H. altissima	0.00–0.10	6.9E-08	1.2E-07	5.0E-08	2.9E-04		
H. altissima	0.10–0.20	5.4E-08	9.8E-08	3.9E-08	2.3E-04		
U. brizantha	0.00–0.10	5.2E-08	9.3E-08	3.8E-08	2.2E-04		
U. brizantha	0.10–0.20	5.6E-08	1.0E-07	4.1E-08	2.4E-04		

[a]The CR by dermal contact was not estimated because of absence of a carcinogenic slope factor.

phytovolatilization (122). This is critical as excessive accumulation of HMs in the human body can lead to respiratory and cardiovascular diseases, and to cognitive impairments (123).

The non-carcinogenic HI considering Zn, V, and Ba was higher for children than for adults, regardless of contact pathways (ingestion, inhalation, dermal contact), treatment and soil layer (Table 7). The average HIing, HIinh and HIdermal values for children in all treatments and soil layers were higher than the risks for adults. Considering the contribution of each exposure pathway (ingestion, inhalation and dermal) to the total risk (HI) sum (calculations not shown), it was observed that the most likely pathway of exposure of adults to HMs in the study area is by ingestion. This is because HQing accounted for approximately 60% of the total HI. For children, a different trend was observed, with about 75% of the total risk (HI) being attributed to HQinh. Among the non-carcinogenic HMs evaluated, Ba was the largest contributor to HI, with contribution rates of 39% for children and 60% for adults.

Regarding the CR (calculated only for Cr), it is possible to observe that CRing and CRinh for adults were similar, while for children the greatest risk observed was CRinh (Table 7). According to USEPA (68), CR values are classified as very low (<1E-06), low (1E-06 to 1E-05), medium (1E-05 to 1E-04), high (1E-04 to 1E-03), and very high (>1E-03). Based on this classification, the CRing values observed in this study are classified as "very low", both for children and adults, regardless of treatment and soil layer (Table 7). In contrast, CRinh values were classified as "low" (regardless of treatments and soil layer) only for adults (Table 7). For children, the CRinh values were classified as "high", irrespective of treatment and soil layer (Table 7). Typically, it is assumed that CR values >1E-04 in soil are not acceptable for children (124), and in all treatment and soil layers this threshold was exceeded (Table 7). Therefore, the CR induced by the presence of Cr in this minesoil should not be overlooked, and special attention must be given to protecting children against Cr in this area.

The human health risk assessment performed in this study revealed that children are more susceptible to the HMs present in the studied minesoil, regardless of whether the risk is carcinogenic or non-carcinogenic. This is in line with Pan et al. (125), who reported that the HI and CR values for children were 7- and 1.7-fold greater, respectively, compared to those for adults in a soil contaminated with HMs. These findings are consistent with a series of studies on human health risk assessment performed in soils contaminated by HMs (126–128). Our findings provide valuable information for the environmental management of risks associated with the recreational use of soils restored over two decades at the Candiota coal mine. Future research in this study site should focus on evaluating the bioavailability of HMs to humans and soil fauna.

4 Conclusions

This work employed a range of environmental, ecological, and health risk indicators to assess the risks associated with HMs in a post-coal minesoil located in southern Brazil, 20 years after restoration with perennial grasses. The average contents of V, Ba, and Cr exceeded local soil quality reference values. The CF and PI consistently indicated that the minesoil is moderately polluted with Ba and Cr and severely polluted with V. Soil depth (0.00–0.10 m and 0.10–0.20 m) did not modify the patterns associated with perennial grass, as HM concentrations, CF, PI, Er, and RI remained within the same classification ranges across depths, indicating a relatively homogeneous distribution of contamination and associated risks within the evaluated soil profile.

Among the perennial grasses evaluated, soils restored with *U. brizantha* generally showed lower CF and PI values for Zn, Ba, V, and Cr compared with *C. dactylon* and *H. altissima*, indicating an association with comparatively lower contamination indices, although HM concentrations and risk classes remained similar among treatments. The *U. brizantha* plots also exhibited a higher abundance of soil fauna, particularly Acari and Hymenoptera, but without corresponding increases in fauna diversity or evenness, and with the absence of earthworms, which were present under the other grasses. Overall, the observed differences among treatments represent associative patterns rather than causal evidence, highlighting the importance of continued monitoring using key bioindicators and further investigation of plant–soil–metal–biota interactions to better understand the ecological functioning of such restored minesoils.

Concerning human health, exposure to the minesoil at this restoration stage offers a high carcinogenic risk for children (CR >1E-04), especially by inhalation, associated with the presence of Cr in the soil, regardless of the perennial grass species used for minesoil restoration. Regarding the non-carcinogenic elements, Ba was the largest contributor to the total HI, with contribution rates of 39% for children and 60% for adults. Overall, our results demonstrate the unsuitability of the study area for general human activities despite 20 years of active restoration of the land. The risk assessment results presented here are unprecedented for the studied site and may serve as a valuable baseline for future monitoring of the quality of this mined land.

Data availability statement

The original contributions presented in the study are included in the article/Supplementary Material, further inquiries can be directed to the corresponding author/s.

Author contributions

JO: Formal Analysis, Writing – original draft, Data curation, Methodology, Project administration, Conceptualization, Supervision, Writing – review & editing. MF: Formal Analysis, Writing – review & editing. OL: Investigation, Writing – review & editing. BB: Data curation, Writing – review & editing, Methodology, Validation, Formal Analysis. AR: Resources, Writing – review & editing, Methodology, Software. CG: Methodology, Visualization, Writing – review & editing, Validation. LP: Writing – review & editing, Methodology. MJ: Writing – review & editing, Investigation. LS: Resources, Data curation, Investigation, Writing – review & editing, Funding acquisition.

Funding

The author(s) declared that financial support was received for this work and/or its publication. The authors received research support from CAPES and CNPq for financial support allowing the realization of this work. Author Lizete Stumpf received research support from the scholarship granted by CNPq (Process No. 18/2024).

Acknowledgments

The authors thank the Companhia Riograndense de Mineração for logistical assistance.

Conflict of interest

The author(s) declared that this work was conducted in the absence of any commercial or financial relationships that could be construed as a potential conflict of interest.

Generative AI statement

The author(s) declared that generative AI was used in the creation of this manuscript.

Any alternative text (alt text) provided alongside figures in this article has been generated by Frontiers with the support of artificial intelligence and reasonable efforts have been made to ensure accuracy, including review by the authors wherever possible. If you identify any issues, please contact us.

Publisher's note

All claims expressed in this article are solely those of the authors and do not necessarily represent those of their affiliated organizations, or those of the publisher, the editors and the reviewers. Any product that may be evaluated in this article, or claim that may be made by its manufacturer, is not guaranteed or endorsed by the publisher.

Supplementary material

The Supplementary Material for this article can be found online at: https://www.frontiersin.org/articles/10.3389/fsoil.2026.1754030/full#supplementary-material.

References

1. Pinto LFS, Stumpf L, Miguel P, Junior LAD, Leidemer JD, Barbosa LS, et al. Reclamation of soils degraded by surface coal mining. In: Soni A, editor. *Mining techniques—Past, present, and future*. London, United Kingdom: IntechOpen (2020). doi: 10.5772/intechopen.93432

2. Chen L, Zhou M, Wang J, Zhang Z, Duan C, Wang X, et al. A global meta-analysis of heavy metal(loid)s pollution in soils near copper mines: Evaluation of pollution level and probabilistic health risks. *Sci Total Environ*. (2022) 835:155441. doi: 10.1016/j.scitotenv.2022.155441

3. Dusengemungu L, Mubemba B, Gwanama C. Evaluation of heavy metal contamination in copper mine tailing soils of Kitwe and Mufulira, Zambia, for reclamation prospects. *Sci Rep*. (2022) 12:11283. doi: 10.1038/s41598-022-15458-2

4. Hou Y, Zhao Y, Lu J, Wei Q, Zang L, Zhao X. Environmental contamination and health risk assessment of potentially toxic trace metal elements in soils near gold mines – A global meta-analysis. *Environ pollut*. (2023) 330:121803. doi: 10.1016/j.envpol.2023.121803

5. Proto M, Courtney R. Is the use of a geotextile a necessary rehabilitation strategy to mitigate tailings contamination in soil cover materials? A 7-year field study. *Ecol Eng*. (2023) 197:107128. doi: 10.1016/j.ecoleng.2023.107128

6. Kabir E, Ray S, Kim K-H, Yoon H-O, Jeon E-C, Kim YS, et al. Current status of trace metal pollution in soils affected by industrial activities. *Sci World J*. (2012) 2012:1–18. doi: 10.1100/2012/916705

7. Alvarez-Fernández A, Díaz-Benito P, Abadía A, López-Millán AF, Abadía J. Metal species involved in long distance metal transport in plants. *Front Plant Sci*. (2014) 5:105. doi: 10.3389/fpls.2014.00105

8. Alidou-Arzika I, Lebrun M, Miard F, Nandillon R, Baycu G, Bourgerie S, et al. Assessment of compost and three biochars associated with *Ailanthus altissima* (Miller) Swingle for lead and arsenic stabilization in a post-mining Technosol. *Pedosphere*. (2021) 31:944–53. doi: 10.1016/S1002-0160(21)60025-5

9. Cui X, Geng Y, Sun R, Xie M, Feng X, Li X, et al. Distribution, speciation and ecological risk assessment of heavy metals in Jinan Iron & Steel Group soils from China. *J Cleaner Production*. (2021) 295:126504. doi: 10.1016/j.jclepro.2021.126504

10. Kou J, Gan Y, Lei S, Meng W, Feng C, Xiao H. Soil health and ecological risk assessment in the typical coal mines on the Mongolian Plateau. *Ecol Indic*. (2022) 142:109189. doi: 10.1016/j.ecolind.2022.109189

11. Sojka M, Jaskuła J. Heavy metals in river sediments: Contamination, toxicity, and source identification—a case study from Poland. *Int J Environ Res Public Health*. (2022) 19:10502. doi: 10.3390/ijerph191710502

12. Arif N, Yadav V, Singh S, Singh S, Ahmad P, Mishra RK, et al. Influence of high and low levels of plant-beneficial heavy metal ions on plant growth and development. *Front Environ Sci*. (2016) 4:69. doi: 10.3389/fenvs.2016.00069

13. Furini A. *Plants and heavy metals*. Germany: Springer Science & Business Media (2012) 86.

14. Kabata-Pendias A, Pendias H. *Trace elements in soils and plants. 3rd ed*. Boca Raton: CRC Press (2001).

15. Wuana RA, Okieimen FE. Heavy metals in contaminated soils: A review of sources, chemistry, risks and best available strategies for remediation. *Int Scholarly Res Notices*. (2011) 2011:e402647. doi: 10.5402/2011/402647

16. Huang Y, Deng M, Wu S, Jan J, Li T, Yang X, et al. A modified receptor model for source apportionment of heavy metal pollution in soil. *J Hazardous Materials*. (2018) 354:161–9. doi: 10.1016/j.jhazmat.2018.05.006

17. Kumar A, Tripti, Raj D, Maiti SK, Maleva M, Borisova G. Soil pollution and plant efficiency indices for phytoremediation of heavy metal(loid)s: Two-decade study (2002–2021). *Metals*. (2022) 12:1330. doi: 10.3390/met12081330

18. Li SQ, Liber K. Influence of different revegetation choices on plant community and soil development nine years after initial planting on a reclaimed coal gob pile in the Shanxi mining area, China. *Sci Total Environ*. (2018) 618:1314–23. doi: 10.1016/j.scitotenv.2017.09.252

19. Urbanowski CK, Kamczyc J, Skorupski M. Does litter decomposition affect mite communities (Acari, Mesostigmata)? A five-year litterbag experiment with 14 tree species in mixed forest stands growing on a post-industrial area. *Geoderma*. (2021) 391:114963. doi: 10.1016/j.geoderma.2021.114963

20. Peng Y, Holmstrup M, Schmidt IK, De Schrijver A, Schelfhout S, Heděnec P, et al. Litter quality, mycorrhizal association, and soil properties regulate effects of tree species on the soil fauna community. *Geoderma*. (2022) 407:115570. doi: 10.1016/j.geoderma.2021.115570

21. Wierzbicka A, Dyderski MK, Kamzcyc J, Rączka G, Jagodziński AM. Responses of soil mite communities (Acari: Oribatida, Mesostigmata) to elemental composition of mosses and pine needles and long-term air pollution in Scots pine (*Pinus sylvestris* L.) stands. *Sci Total Environ*. (2019) 691:284–95. doi: 10.1016/j.scitotenv.2019.07.138

22. Prüss-Üstün A, Wolf J, Corvalán, Carlos F, Bos R, Neira MP. *Preventing disease through healthy environments: a global assessment of the burden of disease from environmental risks*. Geneva, Switzerland: World Health Organization ([amp]] lrm;2016). Available online at: https://iris.who.int/handle/10665/204585 (Accessed June 12, 2024).

23. Xu X, Nie S, Ding H, Fan HF. Environmental pollution and kidney diseases. *Nat Rev Nephrol*. (2018) 14:313–324. doi: 10.1038/nrneph.2018.11

24. Zulfiqar U, Farooq M, Hussain S, Maqsood M, Hussain M, Ishfaq M, et al. Lead toxicity in plants: Impacts and remediation. *J Environ Manage*. (2019) 250:109557. doi: 10.1016/j.jenvman.2019.109557

25. Deng S, Zhang X, Zhu Y, Zhuo R. Recent advances in phyto-combined remediation of heavy metal pollution in soil. *Biotechnol Adv*. (2024) 72:108337. doi: 10.1016/j.bioteChadv.2024.108337

26. Kumar B, Singh UK. Source apportionment of heavy metals and their ecological risk in a tropical river basin system. *Environ Sci pollut Res*. (2018) 25:25443–57. doi: 10.1007/s11356-018-2577-9

27. Verma F, Singh S, Dhaliwal SS, Kumar V, Kumar R, Singh J, et al. Appraisal of pollution of potentially toxic elements in different soils collected around the industrial area. *Heliyon*. (2021) 7:e08122. doi: 10.1016/j.heliyon.2021.e08122

28. Kijowska-Strugała M, Baran A, Szara-Bąk M, Wiejaczka Ł., Prokop P. Soil quality under different agricultural land uses as evaluated by chemical, geochemical and ecological indicators in mountains with high rainfall (Darjeeling Himalayas, India). *J Soils Sediments*. (2022) 22:3041. doi: 10.1007/s11368-022-03258-w

29. Yang J, Sun Y, Wang Z, Gong J, Gao J, Tang S, et al. Heavy metal pollution in agricultural soils of a typical volcanic area: Risk assessment and source appointment. *Chemosphere*. (2022) 304:135340. doi: 10.1016/j.chemosphere.2022.135340

30. Hoque MM, Islam A, Islam ARMT, Pal SC, Mahammad S, Alam E. Assessment of soil heavy metal pollution and associated ecological risk of agriculture-dominated mid-channel bars in a subtropical river basin. *Sci Rep*. (2023) 13:11104. doi: 10.1038/s41598-023-38058-0

31. Gui H, Yang Q, Lu X, Wang H, Gu Q, Delgado Martín J. Spatial distribution, contamination characteristics and ecological-health risk assessment of toxic heavy metals in soils near a smelting area. *Environ Res*. (2023) 222:115328. doi: 10.1016/j.envres.2023.115328

32. Shetty BR, Pai BJ, Salmataj SA, Naik N. Assessment of carcinogenic and non-carcinogenic risk indices of heavy metal exposure in different age groups using Monte Carlo Simulation Approach. *Sci Rep*. (2024) 14:30319. doi: 10.1038/s41598-024-81109-3

33. Xing J, Gao L, He L. Species distribution and concentration pollution of soil heavy metals in coal mine reclamation areas. *Front Environ Sci*. (2022) 10:925074. doi: 10.3389/fenvs.2022.925074

34. Hao H, Zhang M, Wang J, Fu Z, Balaji P, Jiang S. Barium in coal and coal combustion products: distribution, enrichment and migration. *Energy Explor Exploitation*. (2022) 40:889–907. doi: 10.1177/01445987221086981

35. Huang Z, Chen T, Yang Z, Wang Y, Zhou Y, Ding X, et al. Risk assessment and microbial community structure in agricultural soils contaminated by vanadium from stone coal mining. *Chemosphere*. (2023) 310:136916. doi: 10.1016/j.chemosphere.2022.136916

36. FEPAM - State Foundation for Environmental Protection Henrique Luiz Roessler/RS. *Ordinance FEPAM n° 85/2014: Establishment of soil quality reference values (QRV) for nine chemical elements naturally present in the different geomorphological/geological provinces of the State of Rio Grande do Sul* (2014). Available online at: https://www.fepam.rs.gov.br/upload/arquivos/202301/27114351-portaria085-2014.pdf (Accessed June 01, 2024).

37. Stumpf L, Leal OA, Pauletto EA, Pinto LFS, Reis DA, Pinto MAB, et al. Tensile strength and organic matter fractions in aggregates of a grass-covered mined soil under early stage recovery. *Soil Tillage Res*. (2018) 176:69–76. doi: 10.1016/j.still.2017.11.006

38. Fernandez MBG, Leal OA, Junior AP, Islabão LO, Silveira LM, Nogueira HL, et al. First assessment of soil mesofauna, microbiota, and humic substances associations in a minesoil revegetated with four grasses in Brazil: an 18-year field study. *Eur J Soil Biol*. (2023) 118:103533. doi: 10.1016/j.ejsobi.2023.103533

39. Fernandez MBG, Stumpf L, Miguel P, Pinto LFS, Carlos FS, Schubert RN, et al. Biological quality and organic matter dynamics in minesoil at 18 years reclamation with perennial grasses. *Ecol Eng*. (2023) 187:106866. doi: 10.1016/j.ecoleng.2022.106866

40. Fernandez MBG, Leal OA, Islabão GO, Junior AP, Melo TV, Knapp AP, et al. Temporal dynamics of minesoil restoration in Southern Brazil: A two-decade monitoring of soil physical attributes and organic carbon content. *Soil Tillage Res*. (2025) 253:106647. doi: 10.1016/j.still.2025.106647

41. Leal OA, Miguel P, Rodrigues MF, Guimarães RML, Pinto LFS, Silva TP, et al. First validation of the method Visual Evaluation of Soil Structure in coal mining area using a long-term field revegetation experiment as testbed. *Soil Tillage Res*. (2025) 246:106347. doi: 10.1016/j.still.2024.106347

42. Oliveira MS, Leal OA, Fernandez MBG, Brüggemann N, Miguel P, Pinto LFS, et al. Abundance and diversity of mesofauna in relation to minesoil Properties after 14.6 years of revegetation with grasses. *Ecol Eng*. (2025) 214:107578. doi: 10.1016/j.ecoleng.2025.107578

43. Alvares CA, Stape JL, Sentelhas PC, Gonçalves JLM, Sparovek G. Köppen's climate classification map for Brazil. *Meteorologische Z*. (2013) 22:711–28. doi: 10.1127/0941-2948/2013/0507

44. MapBiomas. *Projeto MapBiomas – Mapeamento anual de cobertura e uso da terra no Brasil entre 1985 a 2022* (2023). Available online at: https://brasil.mapbiomas.org/wp-content/uploads/sites/4/2023/09/FACT_port-versao-final.pdf (Accessed June 07, 2024).

45. Stumpf L, Pauletto EA, Pinto LFS. Soil aggregation and root growth of perennial grasses in a constructed clay minesoil. *Soil Tillage Res*. (2016) 161:71–8. doi: 10.1016/j.still.2016.03.009

46. CQFS - Comissão de Química e Fertilidade do Solo. *Manual de adubação e calagem para os estados do Rio Grande do Sul e de Santa Catarina; SBCS-NRS: Brasil. 11th ed*. Porto Alegre: Editora Pallotti (2016). p. 375.

47. Teixeira PC, Donagemma GK, Fontana A, Teixeira WG. *Manual de Métodos de Análise de Solos. 3ª edição Revista e Ampliada*. Brasília: Embrapa (2017). p. 573.

48. USEPA - Environmental Protection Agency (U.S. EPA). *Method 3050B: Acid digestion of sediments, sludges, and soil* (1996). Available online at: https://www.epa.gov/waste/hazard/testmethods/sw846/pdfs/3050b.pdf (Accessed February 03, 2024).

49. Lima FRD, Barbosa AP, Vasques ICF, Oliveira JR, Silva AO, Martins GC, et al. Physiological effects of mercury-contaminated Oxisols on common bean and oat. *Environ Sci pollut Res*. (2020) 1:1. doi: 10.1007/s11356-020-10677-x

50. Oliveira JR, Vasques ICF, Lima FRD, Carvalho GS, Job MTP, De Oliveira TS, et al. Mercury adsorption in tropical soils and zeolite: Characterization by Fourier-transform infrared spectroscopy. *Arch Agron Soil Sci*. (2020) 1:3650340.2020.1845318. doi: 10.1080/03650340.2020.1845318

51. Vasques ICF, Egreja Filho FB, Morais EG, Lima FRD, Oliveira JR, Pereira P, et al. Mercury fractionation in tropical soils: A critical point of view. *Chemosphere*. (2020) 257:127114. doi: 10.1016/j.chemosphere.2020.127114

52. APHA - American Public Health Association. *Standard methods for the examination of water and wastewater. 22nd ed*. Washington, DC: American Public Health Association, American Water Works Association, & Water Environment Federation (2012).

53. Hakanson L. An ecological risk index for aquatic pollution control: A sedimentological approach. *Water Res*. (1980) 14:975–1001. doi: 10.1016/0043-1354(80)90143-8

54. CETESB – Companhia Ambiental do Estado de São Paulo. *Atualização da Lista de Valores Orientadores para Solo e Água Subterrânea*. Governo do Estado de São Paulo, São Paulo: CETESB (2021). Available online at: https://cetesb.sp.gov.br/wp-content/uploads/2021/12/DD-125-2021-E-Atualizacao-dos-Valores-Orientadores-paa-solo-e-aguas-subterraneas.pdf (Accessed December 18, 2024).

55. Nemerow NL. *Stream, lake, estuary, and ocean pollution*. New York, USA: John Wiley & Sons (1991).

56. Keshavarzi A, Kumar V. Ecological risk assessment and source apportionment of heavy metal contamination in agricultural soils of Northeastern Iran. *Int J Environ Health Res*. (2019) 29:1–13. doi: 10.1080/09603123.2018.1555638

57. Zhuang W, Wang Q, Tang L, Liu J, Yue W, Liu Y, et al. A new ecological risk assessment index for metal elements in sediments based on receptor model, speciation, and toxicity coefficient by taking the Nansihu Lake as an example. *Ecol Indic*. (2018) 89:725–37. doi: 10.1016/j.ecolind.2018.02.033

58. Kamani H, Mirzaei N, Ghaderpoori M, Bazrafshan E, Rezaei S, Mahvi AH. Concentration and ecological risk of heavy metal in street dusts of Eslamshahr, Iran. *Hum Ecol Risk Assessment: Int J*. (2017) 24:961–70. doi: 10.1080/10807039.2017.1403282

59. Anderson JM, Ingram JIS. *Tropical soil biology and fertility: A handbook of methods. 2nd Edition*. Wallingford, UK: C.A.B. International (1993). p. 221.

60. Lavelle P, Decaëns T, Aubert M, Barot S, Blouin M, Bureau F, et al. Soil invertebrates and ecosystem services. *Eur J Soil Biol*. (2006) 42:S3–S15. doi: 10.1016/j.ejsobi.2006.10.002

61. Bachelier G. *La Faune des sols: son écologie et son action*. Paris: ORSTOM (1978). Available online at: https://horizon.documentation.ird.fr/exl-doc/pleins_textes/pleins_textes_6/Idt/09691.pdf (Accessed August 12, 2024).

62. Aquino AM, Aguiar-Menezes EL, Queiroz JM. *Recomendações para coleta de artrópodes terrestres por armadilhas de queda ("Pitfall traps")*. Embrapa Seropédica, Rio de Janeiro (2006). p. 8.

63. Gallo D, Nakano O, Silveira Neto S, Carvalho RPL, Batista GC, Berti Filho E, et al. Manual de entomologia agrícola. *São Paulo Ed Agron Ceres*. (1988) 2:649.

64. González G, Seastedt TR. Comparison of the abundance and comparison of litter fauna in tropical and subalpine forests. *Pedobiologia*. (2000) 44:545–55. doi: 10.1078/S0031-4056(04)70070-0

65. USEPA - Environmental Protection Agency (U.S. EPA). *A review of the reference dose (RfD) and reference concentration (RfC) processes*. Washington, DC: Risk Assessment Forum (2002).

66. USEPA - Environmental Protection Agency (U.S. EPA). *Determination of the appropriate FQPA safety factor(s) in tolerance assessment*. Washington, DC: Office of Pesticide Programs (2002).

67. Cui W, Mei Y, Liu S, Zhang X. Health risk assessment of heavy metal pollution and its sources in agricultural soils near Hongfeng Lake in the mining area of Guizhou Province, China. *Front Public Health*. (2023) 11:1276925. doi: 10.3389/fpubh.2023.1276925

68. USEPA - Environmental Protection Agency (U.S. EPA). *A risk assessment–multi way exposure spread sheet calculation tool*. Washington, DC: United States Environmental Protection Agency (1999).

69. Hammer O, Harper D, Ryan P. PAST: paleontological statistics software package for education and data analysis. *Palaeontologia Electronica*. (2001) 4:1–9.

70. Yan A, Wang Y, Tan SN, Yusof MLM, Ghosh S, Chen Z. Phytoremediation: A promising approach for revegetation of heavy metal-polluted land. *Front Plant Sci*. (2020) 11:359. doi: 10.3389/fpls.2020.00359

71. Zhang S, Li H, Wu Z, Post JE, Lanson B, Liu Y, et al. Effects of cobalt doping on the reactivity of hausmannite for As(III) oxidation and As(V) adsorption. *J Environ Sci*. (2022) 122:217–26. doi: 10.1016/j.jes.2022.02.004

72. Kravchenko E, Minkina T, Mandzhieva S, Bauer T, Lacynnik E, Wong MH, et al. Ecological and health risk assessments of heavy metal contamination in soils surrounding a coal power plant. *J Hazardous Materials*. (2025) 484:136751. doi: 10.1016/j.jhazmat.2024.136751

73. Burgueño LE, Pinto LFS, Stumpf L, Piana CFB, Oliveira MS, Quadro MS, et al. Evolution of a technosol cultivated with perennial grass, over 15 years: potential use as carbon sinks. In: *Technologies in mining*. London, UK: IntechOpen (2024). doi: 10.5772/intechopen.1005687

74. Oliveira ML, Ward CR, French D, Hower JC, Querol X, Silva L,FO. Mineralogy and leaching characteristics of beneficiated coal products from Santa Catarina, Brazil. *Int J Coal Geology*. (2012) 94:314–25. doi: 10.1016/j.coal.2011.11.007

75. Bartoňová L, Raclavská H, Najser J. Vanadium – Valuable and toxic element in coal combustion ash: An overview. *Process Saf Environ Prot*. (2023) 172:923–40. doi: 10.1016/j.psep.2023.02.070

76. Xiao X, Yang M, Guo Z, Jiang Z, Liu Y, Cao X. Soil vanadium pollution and microbial response characteristics from stone coal smelting district. *Trans Nonferrous Metals Soc China 25(4)*. (2015) 25:1271–8. doi: 10.1016/s1003-6326(15)63727-x

77. Anirudhan TS, Radhakrishnan PG. Adsorptive performance of an amine-functionalized poly(hydroxyethylmethacrylate)-grafted tamarind fruit shell for Vanadium(V) removal from aqueous solutions. *Chem Eng J*. (2010) 165:142–50. doi: 10.1016/j.cej.2010.09.005

78. Ketris MP, Yudovich YE. Estimations of Clarkes for carbonaceous biolithes: World averages for trace element contents in black shales and coals. *Int J Coal Geology*. (2009) 78:135–48. doi: 10.1016/j.coal.2009.01.002

79. Jiang K, Qi H-W, Hu R-Z. Element mobilization and redistribution under extreme tropical weathering of basalts from the Hainan Island, South China. *J Asian Earth Sci*. (2018) 158:80–102. doi: 10.1016/j.jseaes.2018.02.008

80. Kosmulski M. The pH-dependent surface charging and the points of zero charge. *J Colloid Interface Sci*. (2002) 253:77–87. doi: 10.1006/jcis.2002.8490

81. Dai SF, Ren DY, Chou CL, Finkelman RB, Seredin VV, Zhou YP. Geochemistry of trace elements in Chinese coals: A review of abundances, genetic types, impacts on human health, and industrial utilization. *Int J Coal Geology*. (2012) 94:3–21. doi: 10.1016/j.coal.2011.02.003

82. Silva LFO, Querol X, Boit KM, Fdez-Ortiz SV, Madariaga JM. Brazilian coal mining residues and sulphide oxidation by Fenton's reaction: An accelerated weathering procedure to evaluate possible environmental impact. *J Hazardous Materials*. (2011) 186:516–25. doi: 10.1016/j.jhazmat.2010.11.032

83. Shah P, Strezov V, Nelson PF. Speciation of chromium in Australian coals and combustion products. *Fuel*. (2012) 102:1–8. doi: 10.1016/j.fuel.2012.05.034

84. Javadinejad S, Ostad-Ali-Askari K, Jafary F. Using simulation model to determine the regulation and to optimize the quantity of chlorine injection in water distribution networks. *Modeling Earth Syst Environ*. (2019) 5:1015–23. doi: 10.1007/s40808-019-00587-1

85. Kabata-Pendias A. *Oligoelementos em solos e plantas*. Boca Raton, FL: CRC Press (2010).

86. Zulfiqar U, Haider FU, Ahmad M, Hussain S, Maqsood MF, Ishfaq M, et al. Chromium toxicity, speciation, and remediation strategies in soil-plant interface: A critical review. *Front Plant Sci*. (2023) 13:1081624. doi: 10.3389/fpls.2022.1081624

87. RoyChowdhury A, Sarkar D, Deng Y, Datta R. Assessment of soil and water contamination at the Tab-Simco. *Mine Water Environ*. (2017) 36:248–54. doi: 10.1007/s10230-016-0401-9

88. Niu S, Gao L, Zhao J. Distribution and risk assessment of heavy metals in the Xinzhuangzi reclamation soil from the Huainan coal mining area, China. *Hum Ecol Risk Assessment: Int J*. (2014) 21:900–12. doi: 10.1080/10807039.2014.943572

89. Sutkowska K, Teper L, Czech T, Walker A. Assessment of the condition of soils before planned hard coal mining in Southern Poland: A starting point for sustainable management of fossil fuel resources. *Energies*. (2023) 16:737. doi: 10.3390/en16020737

90. Wang X, Zhou C, Liu G, Dong Z. Transfer of metals from soil to crops in an area near a coal gangue pile in the Guqiao coal mine, China. *Analytical Lett*. (2013) 46:1962–77. doi: 10.1080/00032719.2013.789888

91. Lu L, Liu G, Wang J, Wu Y. Bioavailability and mobility of heavy metals in soil in vicinity of a coal mine from Huaibei, China. *Hum Ecol Risk Assessment: Int J*. (2017) 23:1164–77. doi: 10.1080/10807039.2017.1306431

92. Leal OA, Castilhos RMV, Pinto LFS, Pauletto EA, Lemes ES, Kunde RJ. Initial recovery of organic matter of a grass-covered constructed soil after coal mining. *Rev Bras Ciec do Solo*. (2016) 40:e0150384. doi: 10.1590/18069657rbcs20150384

93. Parrotta L, Guerriero G, Sergeant K, Cai G, Hausman JF. The cell wall of early- and later-diverging plants vs cadmium toxicity: Differences in the response mechanisms. *Front Plant Sci*. (2015) 6:133. doi: 10.3389/fpls.2015.00133

94. Khan SR, Singh SK, Rastogi N. Heavy metal accumulation and ecosystem engineering by two common mine site-nesting ant species: Implications for pollution-level assessment and bioremediation of coal mine soil. *Environ Monit Assess*. (2017) 189:195. doi: 10.1007/s10661-017-5865-y

95. Santos FS, Hernández-Allica J, Becerril JM, Amaral-Sobrinho N, Mazur N, Garbisu C. Chelate-induced phytoextraction of metal polluted soils with Brachiaria decumbens. *Chemosphere*. (2006) 65:43–50. doi: 10.1016/j.chemosphere.2006.03.012

96. Farnezi MMM, Silva EB, Santos LL, Silva AC, Grazziotti PH, Alleoni LRF, et al. Potential of forage grasses in phytoremediation of lead through production of phytoliths in contaminated soils. *Land*. (2023) 12:62. doi: 10.3390/land12010062

97. Pan W, Song Z, Liu H, Müeller K, Yang X, Zhang X, et al. Impact of grassland degradation on soil phytolith carbon sequestration in Inner Mongolian steppe of China. *Geoderma*. (2017) 308:86–92. doi: 10.1016/j.geoderma.2017.08.037

98. Caroli M, Furini A, DalCorso G, Rojas M, Di Sansebastiano GP. Endomembrane reorganization induced by heavy metals. *Plants*. (2020) 9:482. doi: 10.3390/plants9040482

99. Crişan I, Balestrini R, Pagliarani C. The current view on heavy metal remediation: The relevance of the plant interaction with arbuscular mycorrhizal fungi. *Plant Stress*. (2024) 12:100439. doi: 10.1016/j.stress.2024.100439

100. Ullah S, Mahmood S, Ali R, Khan MR, Akhtar K, Depar N. Comparing chromium phyto-assessment in Brachiaria mutica and Leptochloa fusca growing on chromium polluted soil. *Chemosphere*. (2020) 257:128728. doi: 10.1016/j.chemosphere.2020.128728

101. Sundaramoorthy AP, Chidambaram A, Sankar Ganesh K, Unnikannan P, Baskaran L. Chromium stress in paddy: (i) Nutrient status of paddy under chromium stress; (ii) Phytoremediation of chromium by aquatic and terrestrial weeds. *Comptes Rendus Biologies*. (2010) 333:597–607. doi: 10.1016/j.crvi.2010.03.002

102. Malik RN, Husain SZ, Nazir I. Heavy metals contamination and accumulation in soils and wild plant species from industrial areas of Islamabad, Pakistan. *Pakistan J Bot*. (2010) 42:291–301.

103. Visconti D, Fiorentino N, Caporale AG, Stinca A, Adamo P, Motti R, et al. Analysis of native vegetation for detailed characterization of a soil contaminated by tannery waste. *Environ pollut*. (2019) 252:1599–608. doi: 10.1016/j.envpol.2019.06.125

104. Gil-Loaiza J, Field JP, White SA, Csavina J, Felix O, Betterton EA, et al. Phytoremediation reduces dust emissions from metal(loid)-contaminated mine tailings. *Environ Sci Technol*. (2018) 52:5851–8. doi: 10.1021/acs.est.7b05730

105. IARC - International Agency for Research on Cancer. *IARC monographs on the evaluation of the carcinogenic risks to humans: A review of human carcinogens: Arsenic, metals, fibres, and dusts (Vol. 100C)*. Lyon, France: World Health Organization (2012).

106. Pushkar B, Sevak P, Parab S, Nilkanth N. Chromium pollution and its bioremediation mechanisms in bacteria: A review. *J Environ Manage*. (2021) 287:112279. doi: 10.1016/j.jenvman.2021.112279

107. Stanley JA, Arosh JA, Burghardt RC, Banu SK. A fetal whole ovarian culture model for the evaluation of CrVI-induced developmental toxicity during germ cell nest breakdown. *Toxicol Appl Pharmacology 289(1)*. (2015) 289:58–69. doi: 10.1016/j.taap.2015.09.002

108. Agarwal P, Vibhandik R, Agrahari R, Daverey A, Rani R. Role of root exudates on the soil microbial diversity and biogeochemistry of heavy metals. *Appl Biochem Biotechnol*. (2023) 195:1–21. doi: 10.1007/s12010-023-04465-2

109. Lu P, Tan Y, Dai N, Di M, Weng X, Zhan Y, et al. Composition and structure of soil fauna communities and their relationships with environmental factors in copper mine waste rock after re-vegetation. *Global Ecol Conserv*. (2021) 32:e01889. doi: 10.1016/j.gecco.2021.e01889

110. Van Vliet PCJ, Didden WAM, van der Zee S.E.A.T.M., Peijnenburg WJGM. Accumulation of heavy metals by enchytraeids and earthworms in a floodplain. *Eur J Soil Biol*. (2006) 42:S117–26. doi: 10.1016/j.ejsobi.2006.09.005

111. Manu M, Băncilă RI, Mountford OJ, Maruşca T, Blaj VA, Onete M. Soil mite (Acari: Mesostigmata) communities and their relationships with some environmental variables in experimental grasslands from Bucegi Mountains in Romania. *Insects*. (2022) 13:285. doi: 10.3390/insects13030285

112. Miguel P, Stumpf L, Pinto LFS, Pauletto EA, Rodrigues MF, Barboza LS, et al. Physical restoration of a minesoil after 10.6 years of revegetation. *Soil Tillage Res*. (2023) 227:105599. doi: 10.1016/j.still.2022.105599

113. Joimel S, Grard B, Auclerc A, Hedde M, Le Doar´e N, Salmon S, et al. Are Collembola "flying" onto green roofs? *Ecol Eng*. (2018) 111:117–24. doi: 10.1016/j.ecoleng.2017.12.002

114. Colombini G, Watteau F, Auclerc A. Technosol rehabilitation strategies drive soil physico-chemical properties and fauna diversity on a former coking plant area. *Appl Soil Ecol*. (2022) 177:104542. doi: 10.1016/j.apsoil.2022.104542

115. Tang H, Zhu J, Huang SF, Qiu JP. Review on application of earthworm in soil heavy metal pollution and remediation. *Soils*. (2013) 45:17–25. doi: 10.13758/j.cnki.tr.2013.01.001

116. Steffan JJ, Brevik EC, Burgess LC, Cerdà A. The effect of soil on human health: An overview. *Eur J Soil Sci*. (2017) 69:159–71. doi: 10.1111/ejss.12451

117. Brevik EC, Slaughter L, Singh BR, Steffan JJ, Collier D, Barnhart P, et al. Soil and human health: Current status and future needs. *Air Soil Water Res*. (2020) 13:1–9. doi: 10.1177/1178622120934441

118. Kodat M, Tepe Y. A holistic approach to the assessment of heavy metal levels and associated risks in the coastal sediment of Giresun, southeast Black Sea. *Heliyon*. (2023) 9:e16424. doi: 10.1016/j.heliyon.2023.e16424

119. USEPA - Environmental Protection Agency (U.S. EPA). *Exposure factors handbook 2011 edition (Final)*. Washington, DC: National Center for Environmental Assessment, Office of Research and Development (2011). Available online at: https://www.epa.gov/expobox/exposure-factors-handbook (Accessed June 10, 2024).

120. Barceloux DG. Vanadium. *J Toxicology: Clin Toxicol*. (1999) 37:265–78. doi: 10.1081/CLT-100102425

121. Kabata-Pendias A, Szteke B. *Oligoelementos em ambientes abióticos e bióticos (Vol. 2015)*. Boca Raton, FL: CRC Press (2015).

122. ITRC - Interstate Technology & Regulatory Council. *Phytotechnology technical and regulatory guidance and decision trees*. Washington, D.C: Interstate Technology & Regulatory Council, Phytotechnologies Team (2009).

123. Madrigal JM, Persky V, Pappalardo A, Argos M. Association of heavy metals with measures of pulmonary function in children and youth: Results from the National Health and Nutrition Examination Survey (NHANES). *Environ Int*. (2018) 121:871–8. doi: 10.1016/j.envint.2018.10.027

124. Gaurav VK, Sharma C. Estimating health risks in metal contaminated land for sustainable agriculture in peri-urban industrial areas using Monte Carlo probabilistic approach. *Sustain Computing: Inf Syst*. (2020) 28:100310. doi: 10.1016/j.suscom.2019.01.012

125. Pan L, Ma J, Wang X, Hou H. Assessments of levels, potential ecological risk, and human health risk of heavy metals in the soils from a typical county in Shanxi Province, China. *Environ Sci pollut Res*. (2016) 23:19330–40. doi: 10.1007/s11356-016-7044-z

126. Tao XQ, Shen DS, Shentu JL, Long YY, Feng YJ, Shen CC. Bioacessibilidade e risco para a saúde de metais pesados em cinzas provenientes da incineração de diferentes resíduos de lixo eletrônico. *Environ Sci pollut Res*. (2014) 22:3558–69. doi: 10.1007/s11356-014-3657-2

127. Wei X, Gao B, Wang P, Zhou HD, Lu J. Pollution characteristics and health risk assessment of heavy metals in street dusts from different functional areas in Beijing, China. *Ecotoxicology Environ Saf*. (2015) 112:186–92. doi: 10.1016/j.ecoenv.2014.11.005

128. Jia Z, Li S, Wang L. Assessment of soil heavy metals for eco-environment and human health in a rapidly urbanization area of the upper Yangtze Basin. *Sci Rep*. (2018) 8:3256. doi: 10.1038/s41598-018-21569-6